Convergent energy state-dependent antagonistic signalling by CART and NPY modulates the plasticity of forebrain neurons to regulate feeding in zebrafish

Devika S. Bodas[1,†], Aditi Maduskar[1,†], Tarun Kaniganti[1], Debia Wakhloo[1], Akilandeswari Balasubramanian[1], Nishikant Subhedar[1] and Aurnab Ghose[1,*]

Running title: CART-NPY antagonism in feeding circuit plasticity

[1] Indian Institute of Science Education and Research (IISER) Pune, Dr Homi Bhabha Road, Pune 411008, INDIA

[†] These authors contributed equally to this work

[*] Correspondence: Dr. Aurnab Ghose, Indian Institute of Science Education and Research (IISER) Pune, Dr Homi Bhaba Road, Pune 411008, INDIA.

Email: aurnab@iiserpune.ac.in

ABSTRACT

Dynamic re-configuration of circuit function subserves the flexibility of innate behaviours tuned to physiological states. Internal energy stores adaptively regulate feeding-associated behaviours by integrating opposing hunger and satiety signals at the level of neural circuits. Across vertebrate lineages, the neuropeptides CART and NPY have potent anorexic and orexic functions, respectively, and show energy state-dependent expression in interoceptive neurons. However, how the antagonistic activities of these peptides modulate circuit plasticity remain unclear.

Using behavioural, neuroanatomical and activity analysis in adult zebrafish, along with pharmacological interventions, we show that CART and NPY activities converge on a population of neurons in the dorsomedial telencephalon (Dm). While CART facilitates glutamatergic neurotransmission at the Dm, NPY dampens the response to glutamate. In energy-rich states, CART enhances NMDA receptor (NMDAR) function by PKA/PKC mediated phosphorylation of the NR1 subunit of the NMDAR complex. Conversely, starvation triggers NPY-mediated reduction in phosphorylated NR1 via calcineurin activation and inhibition of cAMP production leading to reduced responsiveness to glutamate.

Our data identify convergent integration of CART and NPY inputs by the Dm neurons to generate nutritional state-dependent circuit plasticity that is correlated with the behavioural switch induced by the opposing actions of satiety and hunger signals.

Keywords: Neuropeptide signalling; CART; NPY; feeding behaviour; behavioural flexibility; circuit plasticity, NMDA-R

INTRODUCTION

Adaptive regulation of feeding in response to internal energy needs is critical for survival. Internal sensory systems, located in the periphery and in the central nervous system, monitor energy homeostasis and signal satiety or hunger to the feeding-associated neural circuits. Hunger stimulates feeding circuits to generate motivational states that prioritise feeding and related activities over other behaviours. Conversely, satiety signals suppress the 'feeding drive' facilitating the pursuit of non-feeding-related behaviours. The flexibility of the feeding behaviour – exploiting or abandoning food resources – requires dynamic re-configuring of the activity states of the underlying circuits and the de-regulation of these processes form the basis of eating disorders.

Neuropeptides, acting as hormones or local diffusive modulators convey nutritional state information to the nervous system (van den Pol, 2012). Neuropeptide-based neuromodulation of circuit function, via changes in neuronal intrinsic properties or synaptic efficacy, may allow the same circuit to produce multiple outputs and behavioural outcomes (Nadim and Bucher, 2014). Neuropeptides typically engage G-protein coupled receptors (GPCRs) which, via intracellular signalling, may change circuit properties and extend acute signals of internal needs into long-lasting state changes mediated by biochemical hysteresis. For example, in the rodent arcuate nucleus (Arc), orexigenic neuropeptide ghrelin initiates an AMPK-mediated positive-feedback to potentiate glutamate release for extended periods (Yang et al., 2011). Consequently, several studies have implicated neuropeptides in mediating transitions between distinct behavioural states (Root et al., 2011; Elbaz et al., 2012; Flavell et al., 2013; Betley and Sternson, 2015).

Cocaine- and amphetamine-regulated transcript (CART) and Neuropeptide Y (NPY) are abundantly expressed neuropeptides conserved across vertebrate lineages. Both the neuropeptides have been implicated in a diverse range of physiological functions, including energy homoeostasis and food intake (Lau and Herzog, 2014; Subhedar et al., 2014; Singh et al., 2021)

CART is a potent anorexigenic agent and considered to be an endogenous satiety factor (Kristensen et al., 1998), especially in the framework of the Arc in the hypothalamus (Singh et al., 2021). Expression of CART increases in response to feeding in the Arc (Kristensen et al., 1998) and recent chemogenetic studies underscore the requirement of CART peptide in Arc neurons to inhibit food intake (Farzi et al., 2018). In contrast, hypothalamic NPY is orexigenic, and promotes food intake and energy conservation (Zhang et al., 2019). Starvation increases NPY expression in the Arc (Sainsbury and Zhang, 2010) and NPY-signalling from AgRP-expressing Arc neurons is critical for the sustained maintenance of the feeding drive (Chen et al., 2016).

Within the Arc, the coordinated co-regulation of the AgRP/NPY and the POMC/CART containing neurons in response to signals indicating metabolic states is well documented (Dietrich and Horvath, 2013; Andermann and Lowell, 2017). The physiologically opposing activities of these two populations and their effect on “second -order” neurons that drive satiety is a major regulator of the feeding behaviour (Garfield et al., 2015; Andermann and Lowell, 2017). However, the effect of neuropeptide signalling on “second-order” neurons that presumably re-configure the circuit properties to drive homoeostatic plasticity remains inadequately defined.

In zebrafish, NPY and CART are expressed in several brain areas, including the periventricular hypothalamus (homologous to mammalian Arc; Forlano and Cone,

2007) and the entopenduncular nucleus (EN) (Mathieu et al., 2002; Mukherjee et al., 2012; Yokobori et al., 2012; Akash et al., 2014). Starvation decreases CART mRNA expression in the periventricular hypothalamus and the EN (Nishio et al., 2012; Akash et al., 2014) while increasing NPY expression (Yokobori et al., 2012). Treatment with glucose also increases CART protein expression in the EN (Mukherjee et al., 2012). Further, treatment with NPY increases feeding in zebrafish and is mediated by the NPY Y1 receptor (Yokobori et al., 2012). The zebrafish periventricular hypothalamus and the EN appear to be nutritional state sensitive interoceptive areas regulating energy homeostasis, in part via CART/NPY.

Despite the prominent involvement of CART and NPY in vertebrate energy homeostasis, it remains unclear how their activities re-configure the downstream, “second-order” circuits to meet behavioural demands. In this study, using zebrafish, we show that CART and NPY shape the feeding drive to match the prevailing energy states. The opposing energy state information represented by the two neuropeptides are integrated by a group of forebrain neurons by transforming the antagonistic signalling into dynamic changes in glutamatergic neurotransmission.

109 **MATERIALS AND METHODS**

110 **Animals**

111 Adult, wild-type zebrafish (*Danio rerio*) of both sexes were housed in stand-alone
112 housing systems and maintained on 14hL/10hD cycle. Fish were fed Ziegler feed
113 and live artemia 3 times a day. For calcium activity imaging experiments, adult
114 Tg(NeuroD:GcAMP6f) in the *nacre* background were used. All behavioural assays
115 and activity imaging experiments were performed between 10 am and 5 pm. No
116 randomization methods were used to allocate animals to different experimental
117 groups. The Institutional Animal Ethics Committee approved all the procedures
118 employed in this study. This study was not pre-registered.

119 **Chemicals**

120 The following reagents were administered to the zebrafish brain via
121 intracerebroventricular (icv) delivery. The concentrations indicated reflect the amount
122 delivered by the icv route. Rat CART peptide (55-102) (2 pmol in 1x PBS, Phoenix,
123 Cat. No. 003-62), full length human NPY peptide (10 pmol in 1x PBS, Sigma-Aldrich,
124 Cat. No. N5017), anti-CART antibody (1:500; gift from Drs. Lars Thim and Jes
125 Clausen, Novo Nordisk, Denmark); D -(+)- glucose monohydrate (40 nmol in 1x PBS,
126 glucose; Sigma-Aldrich, Cat. No. 49161), BIBP-3226 (100 pmol in 0.1% DMSO,
127 Sigma-Aldrich, Cat. No. B174), MK801 (0.015 nmol in 1x PBS, Sigma-Aldrich, Cat.
128 No. 77086), AP5 (0.1 nmol in 1x PBS, Tocris, Cat. No. 0106), KT5720 (1.4 pmol in
129 1x PBS, PKAi; Sigma-Aldrich, Cat. No. K3761), GF109206X (1.5 pmol in 1x PBS,
130 PKCi; Tocris, Cat. No. 0741), FK506 (0.13 nmol in 1x PBS, Sigma-Aldrich, Cat. No.
131 F4679), Forskolin (1.2 nmol in 0.1 % ethanol, Sigma-Aldrich, Cat. No. F6886). The
132 following reagents were used for procedures not requiring icv administration. 2-

133 Phenoxy Ethanol (1:2000 in system water, Sigma-Aldrich, Cat. No. P1126), D -(+)-
134 glucose monohydrate (Sigma-Aldrich, Cat. No. 49161), sucrose (Sigma-Aldrich, Cat.
135 No. S9703), paraformaldehyde (Sigma-Aldrich, Cat. No. 158127), poly-L- lysine
136 (Sigma-Aldrich, Cat. No. P8920), normal goat serum (Sigma-Aldrich, Cat. No. 9023),
137 bovine serum albumin (BSA) (SRL Pvt. Ltd., Cat. No. 83803), 1, 1', dioctadecyl-
138 3,3,3', 3'- tetramethylindo-carbocyanineperchlorate (DiI; Invitrogen Cat. No. D3911).

139 **Intracerebroventricular (icv) injections**

140 Fish were anaesthetised in 2-phenoxy ethanol (1:2000). The anaesthetised fish were
141 placed on a cotton bed containing anaesthesia solution to submerge the head of the
142 fish. Icv delivery protocol was modified after Yokogawa et al., 2007. Briefly,
143 pharmacological agent or vehicle was delivered directly into the ventricular space
144 using an 31G needle (Becton Dickinson Insulin Syringe U40 - 31G) attached via a
145 catheter to a 10 µl Hamilton microsyringe. After injection, the fish were returned to
146 their tanks and allowed to recover before proceeding for either behavioural
147 recordings or immunohistochemistry. Unless otherwise indicated, 30 mins following
148 injection the animals were subjected to behavioural task or sacrificed and processed
149 for immunofluorescence studies.

150 **Immunofluorescence**

151 Fish were subjected to icv injection with drug or vehicle and allowed to recover for 30
152 mins. After recovery, fish were anesthetised and craniotomised to expose the dorsal
153 surface of the brain. Samples were fixed in 4% PFA overnight at 4 ^{o}C. After fixation
154 for 12-14hrs (10 hrs for pNR1 staining), brain was dissected and cryoprotected with
155 25% sucrose prior to sectioning. Serial 15-20 µm thick sections of the entire
156 telencephalon were mounted onto lysine coated slides and stored at -40 ^{o}C till

157 further processing. Sections were allowed to dry for 2 hrs and washed with 0.5%
158 Triton X-100 in 1x PBS (PBST) three times for 10 min each.). PBS of the following
159 composition was used: NaCl, 137 mM; KCL, 2.7 mM; Na_2HPO_4, 10 mM; KH_2PO_4 ,1.8
160 mM; pH-7.2. Sections were then blocked using 5% BSA in PBST for 1 hr prior to the
161 addition of primary antibodies and incubated overnight at 4°C. Next day, the washes
162 were repeated and sections blocked in 5% BSA/ 5% HIGS for 1 hr. The following
163 primary antibodies were used in this study: anti-p-ERK (1:700, Cell Signalling
164 technologies, Cat. No. 9101), anti- p-ERK (1:500, Abcam, Cat. No. ab50011), anti-
165 pNR1(Ser-897) (1:70, Millipore, Cat. No. ABN99), anti-Synaptophysin (1:100,
166 Invitrogen, Cat. No. PA1-1043).

167 Secondary antibodies were added and incubated at room temperature (RT) for 2.5
168 hrs in dark. The following secondary antibodies were used: Anti-rabbit Alexa Flour
169 488/568 (1:500, Invitrogen, Cat. No. A-11034/ A-11036) and anti-mouse Alexa Flour
170 488/568 (1:500, Invitrogen, Cat. No. A-11029/A-11031). Sections were washed three
171 times and mounted in media (0.5% N propyl gallate, 70% glycerol ,1M tris pH8.0)
172 containing 4′,6-diamidino-2-phenylindole (DAPI) (Invitrogen, Cat. No. D1306).
173 Sections were observed under Axioimager Z1 (Zeiss) epifluorescence microscope
174 and representative images were acquired using confocal microscope (SP8, Leica or
175 LSM 780, Zeiss). In order to ensure reliable comparisons across different groups and
176 maintain stringency in tissue preparation and staining conditions, all the brain
177 sections were processed concurrently under identical conditions.

178 **Feeding Behaviour**

179 Fish were isolated from home tanks and housed singly in the experimental tank prior
180 to behavioural analysis. Fig. S1 outlines the protocol followed for all feeding
181 behaviour experiments. Briefly, for first two days of habituation, the experimental

182 tanks were moved to the recording chamber and the fish were fed floating, insoluble
183 food pellets (15 ± 5 pellets; Taiyo) for 1 hour before returning to the housing rack.
184 For habituation to injection and handling stress, the fish were anesthetised and
185 delivered mock icv injection (saline, 0.9% NaCl) on day 4 and day 5. Fish were
186 allowed to recover in recording chamber for 1 hour, before returning the tanks to the
187 housing racks. Depending on the experiment, the fish were either starved or given
188 pellet food for 1 hr on these days. Fish were observed on all days of the protocol for
189 any anxious/abnormal behaviour. Fish exhibiting such behaviours were not included
190 for further analysis. On the day of the experiment, fish were anaesthetized and icv
191 injected with appropriate reagents or vehicle. Following a recovery period of 15 mins,
192 floating pellets of food (~15 ± 5) were added to the tank and the behaviour of the fish
193 recorded individually using a video recorder (Sony Handycam DCR SR-47 and DCR
194 SR-20) for an hour. All recordings were conducted under conditions of uniform
195 lighting and temperature. In all experiments, animals deprived of food for 2.5 days
196 are referred to as 'starved' and those that received food as per regular feeding
197 schedule, and used for experiments within one hour of feeding, are referred to as
198 'fed'. The recorded videos were not blinded and the number of biting attempts was
199 counted manually. The data was plotted as the cumulative number of biting attempts
200 displayed during 60 mins.

201 **Calcium imaging**

202 Starved, adult Tg(NeuroD:GcAMP6f) fish were injected with either vehicle or drugs.
203 After 15 min, the fish were anesthetized in ice cold HEPES-based Ringer's solution
204 [NaCl, 134 mM; $MgCl_2$, 1.2 mM; $CaCl_2$, 2.1 mM; KCl, 2.9 mM; HEPES, 10 mM;
205 Sucrose, 10 mM (for glucose-deprivation) or Glucose, 10 mM (to mimic satiety); pH
206 7.2] bubbled with 100% O_2 and craniotomised to dissect the telencephalon. The

207 optic nerves were cut off and the telencephalon was dissected out by cutting just
208 rostral to habenula. The telencephalon was carefully lifted from the base while
209 removing the ventral connections and immediately transferred to Ringer's solution
210 supplemented with 100% O_2.

211 For *ex vivo* whole-brain preparations, starved fish were anesthetised in ice-cold
212 HEPES-based Ringer's solution. First the optic nerves and connections on the
213 ventral side were severed and the whole brain was dissected out by separating it
214 from spinal cord.

215 The intact telencephalon or the whole brain was mounted in 4% low-melt agarose (in
216 50% Ringer's) on to a RC-26 GLP chamber from Warner Instruments (Cat. No.
217 640236). The imaging chamber was mounted onto an upright confocal microscope
218 (Leica TCS SP8 MP) and continuously perfused with HEPES-based Ringer's
219 solution via am VC 8 perfusion system (Warner Instruments, Cat. No.640186)
220 directly triggered by the recording software (Leica). Images were acquired at 9.8 Hz
221 at a resolution of 512 x 300 pixels using a 488 nm laser in the resonant, bi-directional
222 scanning mode and a 25x water-immersion objective (N.A 0.95). Baseline imaging
223 was performed for 1 min before the start of the glutamate stimulation. Glutamate (75
224 μM, in Ringer's buffer) was perfused from the 2nd to 5th mins and subsequently
225 washed out.

226 **Data Analysis**

227 Immunofluorescence: The tissue slices were observed under Axioimager Z1 (Zeiss,
228 20x objective 0.8 NA) with the imaging conditions kept constant across all treatment
229 groups. The number of p-ERK positive cells in Dm were scored manually. To avoid

230 over estimation of cell count due to sectioning, the cell numbers were corrected
231 using Abercrombie's method (Abercrombie, 1946).

232 Average pNR1 intensity per cell in Dm was calculated using IMAGE J. For these
233 experiments, the exposure time and other imaging conditions were kept constant for
234 every sample processed. Each neuron in Dm was selected using manual
235 thresholding on the DAPI filter, and the mean intensity of pNR1 per neuron was
236 calculated using IMAGEJ in-built algorithms. Images were acquired using a 40x
237 objective (1.3 NA) on a SP8 confocal microscope (Leica).

238 Calcium imaging: Measurements of population level calcium activity in Dm were
239 performed using ImageJ where the average GCaMP6f fluorescence in the Dm was
240 calculated for each time point. For this, we manually marked an ROI encompassing
241 the Dm using the wand tool in ImageJ on maximum intensity projection of all the
242 frames. This ROI was then applied to the time lapse series and the baseline
243 fluorescence (F0) estimated by taking the average of fluorescence values of 620
244 frames before the start of glutamate treatment. The relative change in fluorescence
245 ($\Delta F/F0$), was calculated using the formula F-F0/F0, where F stands for the
246 fluorescence value at a given time. The maximum response amplitude, i.e.,
247 maximum $\Delta F/F0$ was determined from the temporal sequence using Microsoft Excel.
248 The total magnitude of the response was calculated by computing the area-under-
249 the-curve (AUC), from start of glutamate treatment to end of the washout period, in
250 the GraphPad Prism ver 8 software.

251 Feeding assay: Videos were analysed manually at 1.5x speed and the number of
252 biting attempts were scored. The data were distributed in bins of 15 mins and
253 cumulative biting attempts were plotted using GraphPad Prism ver 8 software.

254 **Statistical Analysis**

255 Data were tested for normality using the Shapiro-Wilk test in GraphPad Prism 8.
256 Behaviour and immunohistochemical data were subjected to the t-test with Welch's
257 correction or the Mann-Whitney test (for single comparison) and One-Way ANOVA
258 with the Tukey's test or Two-way ANOVA, with Bonferroni's post-hoc analysis (for
259 multiple comparisons). All values are expressed as mean ± SEM of the group in the
260 Results section and differences were considered significant at $p<0.05$. Graphs were
261 plotted using the GraphPad Prism 8.0 software. Data for feeding drive are
262 represented as columns (with error bars marking mean± SEM) of cumulative biting
263 attempts in 15 min bins over a 1-hour period. Change in GCaMP6f fluorescence over
264 time is represented as XY plots with the dark line representing mean and the dotted
265 lines denote the SEM. All data shown as violin plots have the thicker dashed line
266 representing median and dotted lines representing first and third quartile.

267

268 **RESULTS**

269 **CART neuropeptide mediates satiety during energy-rich metabolic states**

270 To quantitatively evaluate the feeding drive of adult zebrafish, we developed a
271 behavioural assay that scores the number of biting attempts made by the animal
272 upon presentation of solid, floating food (see Methods and Fig. S1). On comparing
273 recently fed fish with starved animals, we found that hungry fish made more biting
274 attempts over a period of 1 h (794±57.46; Fig. 1 A) compared to fed animals
275 (338.8±70.4; Fig. 1 A). Analysis of the number of biting attempts across 15 min bins
276 revealed cumulated difference over the 1 h period. To rule out contributions from
277 altered locomotion or stress-induced behaviours, we evaluated animals under fed
278 and starved conditions for locomotion kinematics and indicators of anxiety-
279 associated behaviours but found no change in these parameters (Fig. S2).

280 To directly assess the role of CART neuropeptide in anorexia, we delivered CART
281 peptide (55-102 aa) via the intracerebroventricular (icv) route to the brain of starved
282 fish. Strikingly, exogenous administration of CART directly to the brain was sufficient
283 to induce acute anorexia in starved fish (36.21±14.89; Fig. 1 B) compared to starved
284 animals injected with vehicle (829.4±58.03 Fig. 1 B). However, CART treatment did
285 not induce anxiety-like behaviours or modify locomotion (Fig. S2).

286 To test if central application of glucose resulted in anorexia, glucose was directly
287 introduced via the icv route to the brains of starved fish to mimic energy surfeit
288 conditions and preclude peripheral inputs. In contrast to starved animals
289 (852±133.3), glucose-injected fish displayed a dramatic reduction in biting attempts
290 (221.2±33.67; Fig. 1 C). As CART promotes anorexia (Lau and Herzog, 2014b) and
291 CART peptide expression is sensitive to metabolic states in the zebrafish brains

292 (Mukherjee et al., 2012; Akash et al., 2014), we used an immunoneutralising
293 antibody against the CART peptide to test if endogenous CART signalling mediates
294 the glucose-induced reduction in feeding. Indeed, glucose-induced anorexia in
295 starved animals was alleviated in the presence of CART immunoneutralising
296 antibodies also introduced by the icv route (629.9±79.31; Fig 1 C). CART antibodies
297 on their own did not influence the feeding behaviour (658.4±67.13; Fig 1 C).

298 Collectively, these results establish the role of CART neuropeptide signalling in the
299 zebrafish brain in mediating the reduction in food intake behaviour during energy-rich
300 metabolic states.

301

302 **CART signalling alters the activity of telencephalic Dm neurons**

303 The entopeduncular nucleus (EN) in the ventral telencephalon as well as
304 periventricular hypothalamic nuclei, like the nucleus lateralis tuberis (NLT), show
305 energy-state dependent changes in CART mRNA expression (Akash et al., 2014).
306 Administration of glucose also increased the number of CART peptide expressing
307 cells in the EN and the NLT (Fig. S3; Mukherjee et al., 2012).

308 CART immunofluorescence analysis of transverse sections of the zebrafish
309 telencephalon was used to evaluate the projections from the EN. CART-positive EN
310 soma was found to project to the dorsomedial telencephalon (Dm; Fig S4 A). This is
311 consistent with earlier reports indicating that EN neurons project to the Dm (Turner et
312 al., 2016). We used the lipophilic dye, DiI, to further test if the Dm receives
313 projections from EN and other energy status-responsive interoceptive areas. DiI-
314 positive fibres from the Dm typically extended caudally and ventrally and joined the
315 lateral forebrain bundle. Labelled cells were found in the ipsilateral EN (Fig S4 B,C).

316 Fibres were also found to traced further caudally into the hypothalamus and labelled
317 somata were located in the preglomerular nucleus and the NLT (Fig S4 B,D). This
318 connectivity is consistent with previous reports from teleost fish, including zebrafish
319 (Yáñez et al., 2017). Dual immunostaining for CART peptide and the presynaptic
320 marker synaptophysin revealed significant co-localisation, indicating the presence of
321 CART in presynaptic terminals at the Dm (Fig S4 F). However, no CART expressing
322 somas/somata were detected in the Dm.

323 Collectively, these results demonstrate that CART peptide expression in EN and the
324 periventricular hypothalamus is controlled by metabolic states and these areas send
325 projections to the Dm (Fig. S4 E). This connectivity suggested that Dm neurons
326 could be responsive to energy state-dependent CART activity. To assess the
327 involvement of Dm, we used phosphorylated ERK (p-ERK), a marker of recent
328 neuronal activity (Randlett et al., 2015).

329 Starved fish injected with CART peptide via the icv route had an elevated number of
330 p-ERK positive neurons in the Dm (533.9±89.04) in comparison to starved, vehicle-
331 injected animals (159.5±34.52) (Fig 2 A-C). As these data suggest a CART-mediated
332 increase in neuronal activity in the Dm, we tested if feeding was sufficient to induce
333 neuronal activation of the Dm neurons by comparing starved and recently fed fish
334 (where endogenous levels of CART are high; Fig S3. Remarkably, Dm also shows
335 increased neuronal activity (423.2±26.61) in fed fish as compared to starved controls
336 (180.0±12.42) (Fig 2 D-F). The subpopulation of Dm neurons responding to
337 CART/fed states was limited to a ~ 250 µm region starting from the level of the
338 anterior commissure and extending rostrally (Fig 2 G-I).

339 These findings suggest that enhancement of CART function at the Dm, possibly by
340 the energy state responsive neurons of the EN and the periventricular hypothalamus,

results in increased neuronal activity. However, the possibility of additional inputs from other CART-ergic sources cannot be ruled out

CART modulates NMDAR signalling to regulate the feeding behaviour and the activity of Dm neurons

The dorsal telencephalon of teleosts, including the Dm, is rich in glutamatergic neurons (Aoki et al., 2013) and shows significant binding of labelled kainate and l-glutamate (Tong et al., 1992) implicating glutamatergic neurotransmission. Studies in rodents have previously implicated NMDA receptor (NMDAR)-mediated CART signalling in the context of innate fear processing (Rale et al., 2017) and nociceptive transmission (Chiu et al., 2010) in rat. We investigated NMDAR signalling in CART-mediated regulation of feeding behaviour using NMDAR antagonists. Icv delivery of AP5 (competitive NMDAR antagonist) alone in starved fish showed no difference in biting attempts (845.3±89.82; Fig 3 A) as compared to vehicle controls (812.8±84.38. However, CART-induced anorexia (47.33±11.4) was abrogated when CART peptide and AP5 were co-administered (488.7±42.03; Fig 3 A). Application of the non-competitive NMDAR antagonist, MK801 produced similar results (Fig S5 A).

AP5 was co-injected with CART peptide in starved animals to evaluate the role of NMDAR signalling in modulating the activity of the Dm neurons. Neuronal activity in the Dm, indicated by the number of p-ERK positive neurons, was strongly reduced in CART peptide and AP5-treated fish (165.7±11.87) compared to animals injected with only CART peptide (312±18.2; Fig 3 B). AP5 alone (125.2±6.96) did not influence the number of p-ERK positive Dm neurons as compared to those in vehicle controls

364 (126.7±13.35; Fig 3 B). The application of MK801 produced similar results (Fig S5
365 B).

366 Together these data indicate that NMDAR activity is required for processing CART-
367 induced satiety signals in the Dm neurons.

368

369 **PKC and PKA phosphorylate NR1 to mediate the modulation of NMDAR**
370 **signalling by CART**

371 Protein kinase C (PKC) and Protein kinase A (PKA) mediated phosphorylation of the
372 NR1 subunit of the mammalian NMDAR is known to potentiate NMDAR signalling
373 by increasing the channel opening probability and enhancing calcium permeability
374 (Lan et al., 2001; Skeberdis et al., 2006). PKA and PKC have also been implicated in
375 CART-signalling in *in vitro* experiments (Chiu et al., 2010). We next evaluated PKA
376 and PKC function in CART signalling using specific pharmacological inhibitors of
377 PKA and PKC kinase activity.

378 KT5720 (selective PKA inhibitor, PKAi), when co-injected into the ventricle of starved
379 fish along with CART peptide, alleviated (697.49±105.59) the strong reduction in the
380 number of biting attempts induced by CART peptide alone (30.33±10.61 Fig. 4 A).
381 The inhibitor on its own had no significant effect on the feeding drive
382 (713.92±215.68) as compared to starved control animals (782.9± 71.70; Fig. 4 A).

383 Parallel studies evaluating the activity of Dm neurons revealed a robust suppression
384 of CART-induced neuronal activation in fish co-administered with PKAi and CART
385 peptide (158.1±56.47; Fig. 4 B) compared to those injected with only CART peptide
386 (554.5±82.75; Fig. 4 B).

387 As observed for PKAi, inhibition of PKC by GF109206X (selective PKC inhibitor,
388 PKCi) also reversed the suppression of the feeding drive by CART peptide (489.8±
389 29.38 for PKCi + CART and 29.83±6.76 for CART alone; Fig. 4 C) and abrogated the
390 activation of Dm neurons by CART (247.7±28.99 for PKCi + CART and 464.9± 19.57
391 for CART alone; Fig. 4 D).

392 Together, these data implicate PKA and PKC activity in CART-mediated activation of
393 Dm neurons and satiety. PKC and PKA are known to phosphorylate mouse NR1 at
394 multiple residues, including serine 897 (Chen and Roche, 2007). Specific antibodies
395 against phosphoserine 897 of the mouse NR1 (pNR1) were used to evaluate the
396 status of NR1 phosphorylation in the Dm neurons. While the Dm of CART-treated
397 animals displayed strong pNR1 fluorescence (892.1±5), co-injection of PKAi, PKCi,
398 and CART peptide greatly reduced the pNR1 signal (505.9±2.02) (Fig. 4 E-G).

399 Collectively, these data identify CART signalling mediated phosphorylation of NR1
400 via PKA and PKC. The heightened neuronal activity of Dm neurons could be
401 attributed to the potentiation of NMDAR function driven by NR1 phosphorylation.

402

403 **CART treatment potentiates NMDA receptor function resulting in increased**
404 **sensitivity of Dm neurons to excitatory stimuli**

405 Phosphorylation of NR1 subunit of NMDARs by PKA and PKC is known to enhance
406 NMDAR signalling (Lan et al., 2001; Skeberdis et al., 2006). We speculated that a
407 CART-induced increase in phosphorylation of NMDARs would sensitise and
408 enhance the response of Dm neurons to glutamatergic inputs. We tested this
409 hypothesis directly using the Tg(NeuroD:GCaMP6f) zebrafish, which shows strong
410 expression of the genetically-encoded calcium sensor, GCaMP6f in the Dm. *Ex vivo*

411 preparations of the intact telencephalon were dissected from starved animals treated
412 earlier with either saline or CART via the icv route (see Methods and Fig. 5 A). Dm
413 neurons of vehicle-treated animals failed to respond to glutamate stimulation.
414 However, CART peptide-treated animals showed heightened activity of Dm neurons
415 in response to glutamate. Both the maximum amplitude of the response (0.44±0.09
416 for vehicle control and 3.43±0.6 for CART) and the magnitude (area under the curve)
417 of the response (69.04±15.29 for vehicle control and 522.6±94.66 for CART) was
418 substantially higher in starved animals receiving CART peptide (Fig. 5 B-E). Co-
419 treatment of AP5 along with CART peptide prevented the activation of the Dm
420 neurons by glutamate (maximum amplitude:0.29±0.11 compared to 1.724±0.44 for
421 CART alone; magnitude: 64.76±10.88 compared to 230.7± 41.33 for CART alone)
422 and underscored the involvement of NMDAR signalling (Fig. 5 F-H).

423 To determine if the change in the glutamatergic response of Dm neurons in response
424 to CART required PKA and PKC activity, we co-administered selective PKA and
425 PKC inhibitors along with CART. Interestingly, blocking PKA and PKC activity
426 abolished the CART-induced increased sensitivity of Dm neurons to glutamate (Fig.5
427 I-K). The maximum amplitude of response was reduced to 0.21±0.06
428 (PKAi+PKCi+CART) from 2.48±0.43 (CART alone), and the magnitude if the
429 response dropped from 380.3±75.86 (CART alone) to 33.39±7.71
430 (PKAi+PKCi+CART).

431 Together these data suggest that CART signalling via PKA and PKC sensitizes
432 NMDA receptors in the Dm neurons, possibly via post-translational modification of
433 NR1 subunits, leading to the enhanced activation of these neurons. This CART
434 neuropeptide-mediated response of the Dm neurons may constitute a neural
435 representation of the sated state of the animal.

436

437 **The activity of Dm neurons is tuned to changes in energy states**

438 To assess if Dm exhibits heightened activity in energy-rich metabolic states, we used
439 *ex vivo* whole-brain preparations from starved animals maintained in sucrose (to
440 maintain gluco-deprived conditions). Following initial evaluation of the response of
441 Dm neurons to glutamate stimulation, the preparation was incubated in glucose to
442 mimic energy-rich conditions and re-evaluated for neural activity in response to
443 glutamate stimulation (see Methods and Fig. 6 A).

444 Glutamate stimulation of whole-brains of starved animals maintained in gluco-
445 deprived conditions (pre-glucose) failed to activate Dm neurons (maximum amplitude
446 of response: 0.243±0.1 and magnitude of response: 48.29±14.71; Fig 6 B-D).
447 However, upon incubation of the same whole-brain preparation with 10 mM glucose
448 for 30 mins (post-glucose), the Dm neurons responded strongly to glutamate
449 stimulation (maximum amplitude of response: 2.33±0.29 and magnitude of response:
450 485±48.05; Fig 6 B-D). In control experiments, whole-brain preparations from
451 starved animals were maintained throughout in glucose-free media, including the 30
452 min period between the two glutamate stimulations. In these control experiments,
453 Dm neurons did not respond to glutamatergic stimulation either before (pre-control)
454 or after the 30 min control incubation (post-control; Fig 6 B-D).

455 These experiments indicate that activity in the Dm is tuned to changes in glucose
456 levels in the brain and neuronal activity in Dm is correlated to energy states. As
457 CART levels are sensitive to metabolic states (Fig S3; Mukherjee et al., 2012;
458 Akash et al., 2014), the glucosensitive neurons of the EN and hypothalamus may
459 contribute to elevating endogenous CART signalling at the Dm neurons to mediate

460 this effect. Interestingly, the change in Dm activity appears to be independent of
461 peripheral mediators of energy homeostasis.

462

463 **NPY promotes food intake in zebrafish**

464 Beyond sensing energy sufficiency, interoceptive awareness is also expected involve
465 signals indicating depletion of energy stores. Neuropeptide Y (NPY) is a potent
466 orexigenic neuropeptide (Zhang et al., 2019), which is expressed in the EN and
467 periventricular hypothalamic regions of teleosts, including zebrafish (Mathieu et al.,
468 2002; Mukherjee et al., 2012; Akash et al., 2014; Turner et al., 2016) and regulates
469 the feeding behaviour (Yokobori et al., 2012). We tested if NPY signalling regulated
470 zebrafish feeding drive in a manner obverse to CART.

471 A selective NPY receptor Y1R (Y1R) antagonist, BIBP-3226 (BIBP; Doods et al.,
472 1995; Yokobori et al., 2012; Kaniganti et al., 2021), was administered to starved fish
473 to evaluate endogenous NPY signalling in regulating the feeding drive. Compared to
474 vehicle-injected starved animals (789±69.46), BIBP introduced by the icv route
475 robustly suppressed the biting frequency (144.7±21.57; Fig. 7 A) and is consistent
476 with earlier reports (Yokobori et al., 2012).

477 To evaluate if NPY could increase the feeding drive, we intracerebroventricularly
478 introduced NPY peptide into recently fed fish. As expected, vehicle-injected fed fish
479 made infrequent biting attempts (338.8±70.4) while NPY injected animals showed
480 increased feeding drive (983.7±75.84) that was comparable with starved animals
481 (Fig. 7 B). However, there was no change in locomotion or anxiety-like behaviours in
482 NPY-treated animals (Fig. S2).

483

484 **NPY signalling converges on the Dm neurons to decrease neuronal activity**

485 Increased expression of NPY in response to starvation has been reported in several
486 species (Loh et al., 2015), as also observed in the hypothalamic nuclei of zebrafish
487 (Yokobori et al., 2012). Compared to fed zebrafish, the number of NPY positive
488 neurons increased in the EN and the hypothalamic nucleus recessus lateralis (NRL)
489 of starved animals (Fig. S6 A-F).

490 In transverse slices of the telencephalon, NPY-expressing EN soma was found to
491 project to the Dm (Fig S6 G similar to what was seen for CART-positive EN neurons.
492 EN to Dm projections is consistent with previous reports (Turner et al., 2016).
493 Together with DiI tracing experiments reported earlier (Fig. S4 B-D), the connectivity
494 of periventricular hypothalamic nuclei and the EN to Dm (Fig. S6 H) raises the
495 possibility of NPY signalling also converging on the Dm and opposing CART activity.
496 We tested this possibility by evaluating the activity of the Dm neurons in response to
497 NPY.

498 Icv administration of NPY to recently fed animals reduced the number of p-ERK
499 positive Dm neurons (109.5±4.74) compared to vehicle controls (353.5±49.73; Fig. 7
500 C-E). Thus, the difference in the activity of Dm neurons observed between fed and
501 starved animals (Fig. 2 D-F) can be partially explained by the opposing orexic and
502 anorexic signalling by NPY and CART neuropeptides, respectively.

503 As CART signalling increased the phosphorylation of the NR1 subunit of NMDAR to
504 increase neuronal activity, we tested if the reduction of Dm activity following NPY-
505 treatment was a result of decreased NR1 phosphorylation. Indeed, glucose-
506 stimulated (satiety mimic) pNR1 fluorescence (944.3±2.98) was substantially

507 decreased (478.2±2.03) when NPY peptide was co-injected with glucose into the
508 brain of starved fish (Fig. 7 F-H).

509 These data identify NPY-signalling, originating from the energy state sensitive
510 populations of the hypothalamus and EN under energy poor metabolic states, in
511 modulating zebrafish feeding behaviour. NPY-signalling converges on the Dm
512 neurons, acts antagonistically to CART to reduce NR1 phosphorylation and
513 decreases neuronal activity at the Dm.

514

515 **NPY signalling reduced the glutamate responsiveness of Dm neurons**

516 To directly test if NPY signalling reduced the response of Dm neurons to
517 glutamatergic stimulation, we evaluated the Dm activity in the Tg(NeuroD:GCaMP6f)
518 zebrafish line. *Ex vivo* preparations of the intact telencephalon were dissected from
519 starved animals treated earlier with either glucose (satiety mimic) or glucose and
520 NPY via the icv route.

521 As expected, Dm of glucose injected animals responded to glutamate stimulation
522 (maximum amplitude of response: 0.39±0.09 and magnitude of response:
523 75.45±12.93). However, the response to glutamate was substantially damped in the
524 Dm of fish co-injected with glucose and NPY (maximum amplitude of response:
525 0.13±0.06 and magnitude of response: 28.43±4.7; Fig. 7 I-K).

526 These data show that NPY signalling alters the responsiveness of Dm neurons to
527 glutamate and this altered activity state of Dm may be a neuronal representation of
528 the energy deficit conditions. The orexic NPY signalling and the anorexic activities of
529 the CART neuropeptide converge on the Dm neurons. Dm thus appears to be an

530 important integrative centre whose activity is correlated with the homoeostatic
531 regulation of feeding.

532

533 **Orexic signalling by NPY is mediated by the activation of calcineurin and**
534 **inhibition of adenylyl cyclase**

535 Our data identify PKA and PKC mediated phosphorylation of NR1 in the Dm neurons
536 in response to CART in inducing satiety. Further, NPY signalling appears to oppose
537 CART function, including the dephosphorylation of NR1 (Fig 7 H). Thus, we
538 investigated NPY-induced signalling that could oppose CART function.

539 In mammalian systems, NPY is known to increase the activity of the protein
540 phosphatase calcineurin (PP2B) (Chen et al., 2005; Sajdyk et al., 2008) and
541 calcineurin can dephosphorylate NR1 (Choe et al., 2005).We blocked calcineurin
542 activity using FK506 (calcineurin inhibitor) in NPY peptide-treated fed fish and
543 evaluated their feeding behaviour. FK506 alone (222±57.39) did not show any
544 significant effect on the number of biting attempts as compared to vehicle controls
545 (291.4±79.85; Fig 8 A). However, the co-injection of FK506 along with NPY
546 (368±50.97) reversed NPY induced orexia (954.7±67.55; Fig 8 A).

547 To test if blocking calcineurin activity affects NPY induced reduction in Dm activity,
548 we co-injected FK506 and NPY peptide in fed fish. Treatment with the FK506 alone
549 (299.8±38.11) did not affect the number of p-ERK positive neurons in the Dm of fed
550 fish (409.6±32.62; Fig 8 B). On the other hand, blocking calcineurin activity in NPY
551 treated fish (502.4±56.7) abrogated NPY-induced (111±9.38) reduction in p-ERK
552 positive neurons in Dm.

553 We have demonstrated that NPY function in regulating food intake in zebrafish is via
554 the Y1 receptor (Fig. 7 A). NPY Y1R is G protein receptor that inhibits adenylyl
555 cyclase activity (Molosh et al., 2013). A fall in cAMP production by adenylyl cyclase
556 is expected to reduce the activation of PKA, and PKA is critical for CART signalling
557 (Fig 4 A,B). Therefore, we activated adenylyl cyclase with Forskolin (an adenylyl
558 cyclase agonist) in fed fish co-treated with NPY. Forskolin alone (236±77.40) did not
559 influence the number of biting attempts as compared to vehicle controls
560 (261.8±86.98; Fig. 8 C); however, application of Forskolin in NPY co-injected fed fish
561 reversed (194.7±40.7) NPY induced orexia (929±96.86; Fig. 8 C).

562 Forskolin co-administered along with NPY in fed fish, via the icv route, alleviated
563 (304.1±49.90) NPY-mediated reduction of p-ERK positive neurons in the Dm of fed
564 animals (145.1±23.68; Fig. 8 D). Treatment with forskolin alone (223.8±20.05) was
565 comparable to vehicle-injected fed fish (296.6±56.19; Fig 8 D).

566 Collectively, these experiments demonstrate that orexic NPY signalling is mediated
567 by the downregulation of cAMP activity and upregulation of calcineurin activity, which
568 decreases the activity of Dm neurons via reduced phosphorylation of NR1. NPY-
569 signalling is antagonistic to CART-induced phosphorylation of NR1 and the energy-
570 state dependent expression of CART/NPY results in the bimodal regulation of Dm
571 activity and homoeostatic feeding behaviours.

572

573 **DISCUSSION**

574 The flexibility of innate, motivated behaviours is driven by context-dependent
575 recruitment and outputs of the underlying neural circuits (Sternson, 2013; Flavell et
576 al., 2020). Neuromodulator-based signalling has emerged as a key mechanism
577 facilitating reconfiguration of circuit activity (Lee and Dan, 2012). For instance, state
578 changes between component behaviours in *C. elegans* foraging is regulated by the
579 differential recruitment of circuits by the opposing activities of serotonin and the PDF
580 neuropeptide (Flavell et al., 2013). Neuropeptide activities may also change the
581 response of specific neurons or circuits. Peptidergic modulation of the worm ASH
582 neuron mediates feeding state-dependent nociceptive responses (Ezcurra et al.,
583 2016). Similarly, NPY-signalling regulates the sensitivity of zebrafish olfactory
584 receptor neurons in response to hunger (Kaniganti et al., 2021).

585 Homoeostasis necessitates altering food intake in response to changing energy
586 stores. Therefore, the neural circuits regulating food intake need to be dynamic and
587 responsive to physiological states. Neuropeptidergic signalling may represent energy
588 state information and facilitate biochemical modulation of synaptic transmission to
589 regulate food intake-associated behaviours. Indeed, a diverse and complicated
590 network of peptidergic activity, both peripheral and central, influence the plasticity of
591 neural circuits regulating food intake (Crespo et al., 2014). However, the
592 neuropeptide-induced signalling facilitating the integration of opposing energy state
593 signals to generate appropriate behavioural outputs remain poorly understood.

594 In the mammalian Arc, the POMC/CART-expressing neurons of the Arc release α-
595 MSH onto the MC4R-expressing neurons of the paraventricular hypothalamic
596 nucleus (PVH) to enhance glutamatergic neurotransmission and induce satiety
597 (Fenselau et al., 2017). Conversely, the GABAergic AgRP/NPY neurons on the other

598 hand provide an inhibitory tone onto MC4R-expressing PVH neurons to promote
599 food intake (Fenselau et al., 2017). While opposing inputs from the Arc converge
600 onto the PVH neurons, the intracellular mechanisms recruited by these peptidergic
601 neuromodulators are inadequately characterised.

602 We demonstrate the convergence of antagonistic intracellular signalling mediated by
603 the anorexic neuropeptide CART and the orexic NPY on a zebrafish telencephalic
604 neuronal population to reconfigure its activity. Energy state sensitive expression of
605 the neuropeptides impose opposing biochemical constraints on their target neurons
606 at the dorsal telencephalon via the modulation of NMDAR function and regulate the
607 feeding behaviour.

608 We show that not only do the endogenous activities of CART and NPY modulate the
609 feeding drive, but the intracerebroventricular delivery of these peptides acutely alters
610 food intake in the expected direction. We limit our analysis to intracerebroventricular
611 (icv) delivery of bioactive and pharmacological agents to focus on central activities
612 and avoid potential confounds originating from peripheral inputs. Consistent with
613 earlier work (Subhedar et al., 2011; Mukherjee et al., 2012; Yokobori et al., 2012;
614 Akash et al., 2014), we also find that expression of CART peptide increases, under
615 energy-rich conditions, in energy state interoceptive regions of the periventricular
616 hypothalamus and the EN of zebrafish while NPY expression increases upon
617 starvation.

618 Our anatomical analysis indicated that the neurons of the periventricular
619 hypothalamus and the EN send peptidergic projections to the Dorsomedial
620 telencephalon (Dm) and suggests that the latter population may be the target for
621 CART or NPY, under different metabolic states. The connectivity observed in our
622 tracing studies is in line with observations reported in other teleosts (Kanwal et al.,

623 1988), including zebrafish (Turner et al., 2016; Yáñez et al., 2017). Thus, our
624 subsequent studies focussed on the neuronal activity at the Dm, in response to
625 CART and NPY.

626 Using p-ERK as a readout of recent neuronal activity and calcium imaging of a
627 genetically encoded calcium sensor, we found that energy-rich states resulting from
628 recent feeding (and consequent increase in endogenous CART neuropeptide) or
629 exogenous application of CART peptide to the brain led to heightened activity of the
630 Dm neurons. The increased activity of the Dm neurons was found to be NMDAR
631 dependent and blocking NMDAR signalling reduced Dm activity and CART-mediated
632 anorexia.

633 Studies in rodents have previously reported the involvement of NMDA receptors in
634 the regulation of food intake. Under satiety conditions, NMDA receptors in the
635 hindbrain are required for CCK induced reduction of food intake (Wright et al., 2011).
636 NMDAR function has also been implicated in leptin (Neyens et al., 2020) and
637 PACAP (Resch et al., 2014) mediated reduction in food intake. Furthermore,
638 NMDAR activity in the lateral hypothalamus regulates food intake in hungry animals
639 (Stanley et al., 2011), while it is necessary for the activity of the AgRP-expressing
640 neurons to establish the starvation state (Liu et al., 2012). In addition, CART function
641 in processing innate fear in the central amygdala (Rale et al., 2017) and nociception
642 by sensory neurons (Chiu et al., 2010) also involve NMDAR function and may
643 represent a common modality in CART signalling.

644 Further investigations identified PKA and PKC activities in mediating CART induced
645 anorexia since inhibiting the activity of either kinases led to the restoration of food
646 intake and decreased neuronal activation in the Dm. Using phosphospecific NR1

647 antibodies we found that CART induced activation of PKA and PKC results in
648 phosphorylation of NR1 on specific residues.

649 Phosphorylation of NR1 by PKC and PKA has been known to enhance NMDAR
650 signalling by increasing both the Ca^{2+} permeability (Skeberdis et al., 2006) and the
651 opening probability of the receptor complex (Lan et al., 2001). Thus CART-induced
652 phosphorylation is likely to increase the responsiveness of Dm neurons to
653 glutamatergic inputs and is consistent with our results showing heightened calcium
654 response of Dm neurons upon stimulation by glutamate.

655 The modulation of Dm activity by endogenous CART release in response to energy-
656 rich conditions was demonstrated using calcium imaging of *ex vivo* whole-brain
657 preparations where the inputs from the hypothalamus and EN are preserved. Brains
658 isolated from starved animals (low endogenous CART and high endogenous NPY)
659 failed to respond to glutamate when maintained under glucose deprived conditions.
660 However, incubation with glucose restored glutamate responsiveness and suggests
661 altered inputs (including CART) from the glucose-sensing interoceptive areas. While
662 this response may involve modulatory inputs to the Dm not limited to CART, it is
663 consistent with our observations of CART function. Importantly, as the experimental
664 preparation precludes peripheral signals of energy state, the modulation of Dm
665 activity appears to be primarily driven by neuronal inputs.

666 NPY containing neurons of the EN and periventricular hypothalamus also project to
667 the Dm. Thus, the Dm neurons could function as a common substrate for orexic and
668 anorexic inputs and their activity could be dynamically tuned to the prevailing energy
669 states. Indeed, both starvation and exogenous application of NPY to fed fish (low
670 levels of endogenous NPY) led to a reduction in Dm activity with a concomitant
671 increase in the feeding drive.

672 Our investigation reveals that NPY opposes CART-mediated elevation of NR1
673 phosphorylation and consequent increase in Dm activity and anorexia by reducing
674 cAMP production (thereby reducing PKA activation) and activating the phosphatase
675 calcineurin. Our observations are consistent with NPY-mediated activation of
676 calcineurin (Chen et al., 2005; Sajdyk et al., 2008) and calcineurin mediated
677 dephosphorylation of NR1(Choe et al., 2005). Further, NPY Y1R mediated reduction
678 in cAMP and PKA has been shown to decrease NMDA-mediated postsynaptic
679 currents (Molosh et al., 2013) in the neurons of the basolateral amygdala.

680 Our data suggest that Dm neurons are modulated by the opposing activities of CART
681 and NPY to achieve two distinct activity states (Fig. 8 E). Dm neurons, in zebrafish,
682 may represent “second order” neurons, immediately downstream of the
683 interoceptive, “first order” population in the hypothalamus and EN. While our
684 experiments are unable to distinguish whether the same individual neurons respond
685 differentially to CART and NPY, the tight correlation of Dm activity with alterations in
686 food intake behaviour suggest a pivotal role for Dm neurons in regulating energy
687 homoeostasis (Fig. 8 E). A major limitation in delineating CART function has been
688 the lack of well characterised receptors and selective pharmacology. This drawback
689 has limited our analysis of Dm neurons. However, collateral evidence from the
690 gustatory systems also underscores the role of Dm in food intake. In a range of
691 teleosts, the preglomerular tertiary gustatory nucleus is reciprocally connected to the
692 Dm and Dc regions of the telencephalon (Kanwal et al., 1988; Kato et al.,
693 2012).Though the downstream targets of the Dm relevant to the feeding drive are
694 unknown, it appears CART/NPY activities modulate the responsiveness of the Dm to
695 glutamatergic inputs to release or inhibit food intake.

696 The Dm is considered to be homologous to the mammalian amygdaloid complex
697 (Wullimann and Mueller, 2004; Porter and Mueller, 2020). Several recent reports
698 identify the mammalian amygdalar complex in the regulation of feeding behaviours
699 (Padilla et al., 2016; Kim et al., 2017; Izadi and Radahmadi, 2021). Consistent with
700 our findings, the amygdala receives projections from both the NPY and CART
701 neurons of the hypothalamic Arc (Hwang and Lee, 2018) and employs NPY Y1
702 mediated signalling to increase the food intake (Padilla et al., 2016). Additionally,
703 projections from dopamine receptor-positive neurons in prefrontal cortex are known
704 to activate medial BLA to increase food intake (Land et al., 2014). The amygdala is
705 also involved in hindbrain satiety circuits, where PKC-δ+ neurons in the central
706 amygdala (CeA) integrate multiple anorexigenic signals to inhibit food intake (Cai et
707 al., 2014). Conversely, Htr2a+ neurons of the CeA have been shown to stimulate
708 food intake (Douglass et al., 2017). In addition, several anorexigenic
709 neuromodulators, when administered to the CeA have been shown to affect food
710 intake (Fekete et al., 2007; Beckman et al., 2009; Kovács et al., 2012). A recent
711 study has identified appetitive information specific projections from the BLA to the
712 CeA and isolated specific CeA subpopulations that differentially mediate fear
713 processing and feeding-associated behaviours (Kim et al., 2017).

714 While the microcircuitry and the diversity of neuronal subtypes in the zebrafish Dm
715 remain unknown, the feeding regulation-associated CART/NPY-responsive neurons
716 could be distinct from those processing emotions. Consistent with this, no difference
717 in anxiety-like behaviours was seen in fish under fed and starved states or treated
718 with either of the neuropeptides (Fig. S2). The CART/NPY-responsive neurons are a
719 subpopulation restricted to a specific region of the Dm - starting at the level of the
720 anterior commissure and extending 250 μm rostrally (Fig. 2 G-I). Identification of

721 neuronal subtypes within the Dm and development of intersectional genetics will be
722 critical in characterising the CART/NPY-responsive microcircuits in the future.

723 This study investigates neural mechanisms mediating the opposing activities of the
724 neuropeptides CART and NPY in regulating the feeding drive in zebrafish and
725 identifies plasticity in a group of neurons in the zebrafish forebrain. CART and NPY
726 inputs converge on Dm neurons to antagonistically modulate NMDAR function,
727 resulting in an energy state-dependent alteration in glutamatergic neurotransmission
728 that is tightly correlated with the behavioural switch in food intake.

729

730 **REFERENCES**

731 Abercrombie, M. (1946). Estimation of nuclear population from microtome sections.
732 Anat. Rec. *94*, 239–247.

733 Akash, G., Kaniganti, T., Tiwari, N.K., Subhedar, N.K., and Ghose, A. (2014).
734 Differential distribution and energy status-dependent regulation of the four CART
735 neuropeptide genes in the zebrafish brain. J. Comp. Neurol. *522*, 2266–2285.

736 Andermann, M.L., and Lowell, B.B. (2017). Toward a Wiring Diagram Understanding
737 of Appetite Control. Neuron *95*, 757–778.

738 Aoki, T., Kinoshita, M., Aoki, R., Agetsuma, M., Aizawa, H., Yamazaki, M.,
739 Takahoko, M., Amo, R., Arata, A., Higashijima, S. ichi, et al. (2013). Imaging of
740 neural ensemble for the retrieval of a learned behavioral program. Neuron *78*, 881–
741 894.

742 Atasoy, D., and Sternson, S.M. (2016). Functional and Anatomical Dissection of
743 Feeding Circuits. Neuroendocrinol. Appet. 112–133.

744 Beckman, T.R., Shi, Q., Levine, A.S., and Billington, C.J. (2009). Amygdalar opioids
745 modulate hypothalamic melanocortin-induced anorexia. Physiol. Behav. *96*, 568–
746 573.

747 Betley, J.N., and Sternson, S.M. (2015). Applying the Brakes: When to Stop Eating.
748 Neuron *88*, 440–441.

749 Cai, H., Haubensak, W., Anthony, T.E., and Anderson, D.J. (2014). Central
750 amygdala PKC-δ+ neurons mediate the influence of multiple anorexigenic signals.
751 Nat. Neurosci. *17*, 1240–1248.

752 Carter, M.E., Soden, M.E., Zweifel, L.S., and Palmiter, R.D. (2013). Genetic
753 identification of a neural circuit that suppresses appetite. Nature *503*, 111–114.

754 Chen, B.S., and Roche, K.W. (2007). Regulation of NMDA receptors by
755 phosphorylation. Neuropharmacology *53*, 362–368.

756 Chen, M., Li, X., Dong, Q., Li, Y., and Liang, W. (2005). Neuropeptide Y induces

757 cardiomyocyte hypertrophy via calcineurin signaling in rats. Regul. Pept. *125*, 9–15.

758 Chen, Y., Lin, Y.C., Kuo, T.W., and Knight, Z.A. (2015). Sensory Detection of Food
759 Rapidly Modulates Arcuate Feeding Circuits. Cell *160*, 829–841.

760 Chen, Y., Lin, Y., Zimmerman, C.A., Essner, R.A., and Knight, Z.A. (2016). Hunger
761 neurons drive feeding through a sustained , positive reinforcement signal. 1–21.

762 Chiu, H.Y., Lin, H.H., and Lai, C.C. (2010). Cocaine- and amphetamine-regulated
763 transcript (CART) peptide activates ERK pathways via NMDA receptors in rat spinal
764 cord dorsal horn in an age-dependent manner. Regul. Pept. *164*, 90–96.

765 Choe, E.S., Shin, E.H., and Wang, J.Q. (2005). Inhibition of protein phosphatase 2B
766 upregulates serine phosphorylation of N-methyl-d-aspartate receptor NR1 subunits
767 in striatal neurons in vivo. Neurosci. Lett. *384*, 38–43.

768 Crespo, C.S., Cachero, A.P., Jiménez, L.P., Barrios, V., and Ferreiro, E.A. (2014).
769 Peptides and food intake. Front. Endocrinol. (Lausanne). *5*, 1–13.

770 Dietrich, M.O., and Horvath, T.L. (2013). Hypothalamic control of energy balance :
771 insights into the role of synaptic plasticity. Trends Neurosci. *36*, 65–73.

772 Doods, H.N., Wienen, W., Entzeroth, M., Rudolf, K., Eberlein, W., Engel, W., and
773 Wieland, H.A. (1995). Pharmacological characterization of the selective nonpeptide
774 neuropeptide Y Y1 receptor antagonist BIBP 3226. J. Pharmacol. Exp. Ther. *275*,
775 136–142.

776 Douglass, A.M., Kucukdereli, H., Ponserre, M., Markovic, M., Gründemann, J.,
777 Strobel, C., Alcala Morales, P.L., Conzelmann, K.K., Lüthi, A., and Klein, R. (2017).
778 Central amygdala circuits modulate food consumption through a positive-valence
779 mechanism. Nat. Neurosci. *20*, 1384–1394.

780 Elbaz, I., Yelin-Bekerman, L., Nicenboim, J., Vatine, G., and Appelbaum, L. (2012).
781 Genetic ablation of hypocretin neurons alters behavioral state transitions in
782 zebrafish. J. Neurosci. *32*, 12961–12972.

783 Ezcurra, X.M., Walker, X.D.S., Beets, I., Swoboda, X.P., and Schafer, W.R. (2016).
784 Neuropeptidergic Signaling and Active Feeding State Inhibit Nociception in

785 Caenorhabditis elegans. *36*, 3157–3169.

786 Farzi, A., Lau, J., Ip, C.K., Qi, Y., Shi, Y.C., Zhang, L., Tasan, R., Sperk, G., and
787 Herzog, H. (2018). Arcuate nucleus and lateral hypothalamic cart neurons in the
788 mouse brain exert opposing effects on energy expenditure. Elife *7*, 1–27.

789 Fekete, É.M., Bagi, É.E., Tóth, K., and Lénárd, L. (2007). Neuromedin C
790 microinjected into the amygdala inhibits feeding. Brain Res. Bull. *71*, 386–392.

791 Fenselau, H., Campbell, J.N., Verstegen, A.M.J., Madara, J.C., Xu, J., Shah, B.P.,
792 Resch, J.M., Yang, Z., Mandelblat-cerf, Y., Livneh, Y., et al. (2017). A rapidly acting
793 glutamatergic ARC → PVH satiety circuit postsynaptically regulated by a -MSH. *20*.

794 Flavell, S.W., Pokala, N., Macosko, E.Z., Albrecht, D.R., Larsch, J., and Bargmann,
795 C.I. (2013). Serotonin and the neuropeptide PDF initiate and extend opposing
796 behavioral states in C. Elegans. Cell *154*, 1023–1035.

797 Flavell, S.W., Raizen, D.M., and You, Y.J. (2020). Behavioral states. Genetics *216*,
798 315–332.

799 Forlano, P.M., and Cone, R.D. (2007). Conserved neurochemical pathways involved
800 in hypothalamic control of energy homeostasis. J. Comp. Neurol. *505*, 235–248.

801 Garfield, A.S., Li, C., Madara, J.C., Shah, B.P., Webber, E., Steger, J.S., Campbell,
802 J.N., Gavrilova, O., Lee, C.E., Olson, D.P., et al. (2015). A neural basis for
803 melanocortin-4 receptor–regulated appetite. Nat. Neurosci. *18*, 863–871.

804 Horvath, T.L., and Diano, S. (2004). The floating blueprint of hypothalamic feeding
805 circuits. Nat. Rev. Neurosci. *5*, 662–667.

806 Hwang, Y.G., and Lee, H.S. (2018). Neuropeptide Y (NPY) or cocaine- and
807 amphetamine-regulated transcript (CART) fiber innervation on central and medial
808 amygdaloid neurons that project to the locus coeruleus and dorsal raphe in the rat.
809 Brain Res. *1689*, 75–88.

810 Izadi, M.S., and Radahmadi, M. (2021). Overview of the central amygdala role in
811 feeding behaviour. Br. J. Nutr. 1–23.

812 Kaniganti, T., Deogade, A., Maduskar, A., Mukherjee, A., Guru, A., Subhedar, N.,
813 and Ghose, A. Sensitivity of olfactory sensory neurons to food cues is tuned to
814 nutritional states by Neuropeptide Y signaling. J. Neurochem.
815 (doi: 10.1111/jnc.15488).

816 Kanwal, J.S., Finger, T.E., and Caprio, J. (1988). Forebrain connections of the
817 gustatory system in ictalurid catfishes. J. Comp. Neurol. *278*, 353–376.

818 Kato, T., Yamada, Y., and Yamamoto, N. (2012). Ascending gustatory pathways to
819 the telencephalon in goldfish. J. Comp. Neurol. *520*, 2475–2499.

820 Kim, J., Zhang, X., Muralidhar, S., LeBlanc, S.A., and Tonegawa, S. (2017).
821 Basolateral to Central Amygdala Neural Circuits for Appetitive Behaviors. Neuron *93*,
822 1464-1479.e5.

823 Kovács, A., László, K., Gálosi, R., Tóth, K., Ollmann, T., Péczely, L., and Lénárd, L.
824 (2012). Microinjection of RFRP-1 in the central nucleus of amygdala decreases food
825 intake in the rat. Brain Res. Bull. *88*, 589–595.

826 Kristensen, P., Judge, M.E., Thim, L., Ribel, U., Christjansen, K.N., Wulff, B.S.,
827 Clausen, J.T., Jensen, P.B., Madsen, O.D., Vrang, N., et al. (1998). Hypothalamic
828 CART is a new anorectic peptide regulated by leptin. Nature *393*, 72–76.

829 Lan, J.Y., Skeberdis, V.A., Jover, T., Grooms, S.Y., Lin, Y., Araneda, R.C., Zheng,
830 X., Bennett, M. V, and Zukin, R.S. (2001). Protein kinase C modulates NMDA
831 receptor trafficking and gating. Nat. Neurosci. *4*, 382–390.

832 Land, B.B., Narayanan, N.S., Liu, R.-J., Gianessi, C.A., Brayton, C.E., M Grimaldi,
833 D., Sarhan, M., Guarnieri, D.J., Deisseroth, K., Aghajanian, G.K., et al. (2014).
834 Medial prefrontal D1 dopamine neurons control food intake. Nat. Neurosci. *17*, 248–
835 253.

836 Lau, J., and Herzog, H. (2014). CART in the regulation of appetite and energy
837 homeostasis. Front. Neurosci. *8*, 313.

838 Lee, S.H., and Dan, Y. (2012). Neuromodulation of Brain States. Neuron *76*, 209–
839 222.

840 Lin, H.H., Chiu, H.Y., and Lai, C.C. (2005). Potentiation of spinal N-methyl-D-
841 aspartate-mediated nociceptive transmission by cocaine-regulated and
842 amphetamine-regulated transcript peptide in rats. Neuroreport *16*, 253–257.

843 Liu, T., Kong, D., Shah, B.P., Ye, C., Koda, S., Saunders, A., Ding, J.B., Yang, Z.,
844 Sabatini, B.L., and Lowell, B.B. (2012). Fasting Activation of AgRP Neurons
845 Requires NMDA Receptors and Involves Spinogenesis and Increased Excitatory
846 Tone. Neuron *73*, 511–522.

847 Loh, K., Herzog, H., and Shi, Y.C. (2015). Regulation of energy homeostasis by the
848 NPY system. Trends Endocrinol. Metab. *26*, 125–135.

849 Mathieu, M., Tagliafierro, G., Bruzzone, F., and Vallarino, M. (2002). Neuropeptide
850 tyrosine-like immunoreactive system in the brain, olfactory organ and retina of the
851 zebrafish, Danio rerio, during development. Dev. Brain Res. *139*, 255–265.

852 Molosh, A.I., Sajdyk, T.J., Truitt, W.A., Zhu, W., Oxford, G.S., and Shekhar, A.
853 (2013). NPY Y1 Receptors Differentially Modulate GABAA and NMDA Receptors via
854 Divergent Signal-Transduction Pathways to Reduce Excitability of Amygdala
855 Neurons. Neuropsychopharmacology *38*, 1352–1364.

856 Mukherjee, A., Subhedar, N.K., and Ghose, A. (2012). Ontogeny of the cocaine- and
857 amphetamine-regulated transcript (CART) neuropeptide system in the brain of
858 zebrafish, Danio rerio. J. Comp. Neurol. *520*, 770–797.

859 Nadim, F., and Bucher, D. (2014). Neuromodulation of neurons and synapses. Curr.
860 Opin. Neurobiol. *29*, 48–56.

861 Neyens, D., Zhao, H., Huston, N.J., Wayman, G.A., Ritter, R.C., and Appleyard, S.M.
862 (2020). Leptin sensitizes NTS neurons to vagal input by increasing postsynaptic
863 NMDA receptor currents. J. Neurosci. *40*, 7054–7064.

864 Nishio, S.-I., Gibert, Y., Berekelya, L., Bernard, L., Brunet, F., Guillot, E., Le Bail, J.-
865 C., Sánchez, J.A., Galzin, A.M., Triqueneaux, G., et al. (2012). Fasting Induces
866 CART Down-Regulation in the Zebrafish Nervous System in a Cannabinoid Receptor
867 1-Dependent Manner. Mol. Endocrinol. *26*, 1316–1326.

868 Padilla, S.L., Qiu, J., Soden, M.E., Sanz, E., Nestor, C.C., Barker, F.D., Quintana, A.,
869 Zweifel, L.S., Rønnekleiv, O.K., Kelly, M.J., et al. (2016). Agouti-related peptide
870 neural circuits mediate adaptive behaviors in the starved state. Nat. Neurosci. *19*,
871 734–741.

872 van den Pol, A.N. (2012). Neuropeptide Transmission in Brain Circuits. Neuron *76*,
873 98–115.

874 Porter, B.A., and Mueller, T. (2020). The Zebrafish Amygdaloid Complex –
875 Functional Ground Plan, Molecular Delineation, and Everted Topology. Front.
876 Neurosci. *14*.

877 Rale, A., Shendye, N., Bodas, D.S., Subhedar, N., and Ghose, A. (2017). CART
878 neuropeptide modulates the extended amygdalar CeA-vBNST circuit to gate
879 expression of innate fear. Psychoneuroendocrinology *85*, 69–77.

880 Randlett, O., Wee, C.L., Naumann, E.A., Nnaemeka, O., Schoppik, D., Fitzgerald,
881 J.E., Portugues, R., Lacoste, A.M.B., Riegler, C., Engert, F., et al. (2015). Whole-
882 brain activity mapping onto a zebrafish brain atlas. Nat. Methods *12*, 1039–1046.

883 Resch, J.M., Maunze, B., Phillips, K.A., and Choi, S. (2014). Inhibition of food intake
884 by PACAP in the hypothalamic ventromedial nuclei is mediated by NMDA receptors.
885 Physiol. Behav. *133*, 230–235.

886 Root, C.M., Ko, K.I., Jafari, A., and Wang, J.W. (2011). Presynaptic facilitation by
887 neuropeptide signaling mediates odor-driven food search. Cell *145*, 133–144.

888 Sainsbury, A., and Zhang, L. (2010). Role of the arcuate nucleus of the
889 hypothalamus in regulation of body weight during energy deficit. Mol. Cell.
890 Endocrinol. *316*, 109–119.

891 Sajdyk, T.J., Johnson, P.L., Leitermann, R.J., Fitz, S.D., Dietrich, A., Morin, M.,
892 Gehlert, D.R., Urban, J.H., and Shekhar, A. (2008). Neuropeptide Y in the Amygdala
893 Induces Long-Term Resilience to Stress-Induced Reductions in Social Responses
894 But Not Hypothalamic-Adrenal-Pituitary Axis Activity or Hyperthermia. J. Neurosci.
895 *28*, 893–903.

Singh, A., de Araujo, A.M., Krieger, J.P., Vergara, M., Ip, C.K., and de Lartigue, G. (2021). Demystifying functional role of cocaine- and amphetamine-related transcript (CART) peptide in control of energy homeostasis: A twenty-five year expedition. Peptides *140*, 170534.

Skeberdis, V.A., Chevaleyre, V., Lau, C.G., Goldberg, J.H., Pettit, D.L., Suadicani, S.O., Lin, Y., Bennett, M.V.L., Yuste, R., Castillo, P.E., et al. (2006). Protein kinase A regulates calcium permeability of NMDA receptors. Nat. Neurosci. *9*, 501–510.

Stanley, B.G., Urstadt, K.R., Charles, J.R., and Kee, T. (2011). Glutamate and GABA in lateral hypothalamic mechanisms controlling food intake. Physiol. Behav. *104*, 40–46.

Sternson, S.M. (2013). Hypothalamic survival circuits: Blueprints for purposive behaviors. Neuron *77*, 810–824.

Subhedar, N., Barsagade, V.G., Singru, P.S., Thim, L., and Clausen, J.T. (2011). Cocaine- and Amphetamine-Regulated Transcript Peptide (CART) in the Telencephalon of the Catfish , Clarias gariepinus : Distribution and Response to Fasting , 2-Deoxy-D-glucose , Glucose , Insulin , and Leptin Treatments. *1300*, 1281–1300.

Subhedar, N.K., Nakhate, K.T., Upadhya, M.A., and Kokare, D.M. (2014). CART in the brain of vertebrates: Circuits, functions and evolution. Peptides *54*, 108–130.

Tong, C.-K., Pan, M.-P., and Chang, Y.-C. (1992). Characterization of l-glutamate and kainate binding sites in the brain of a freshwater fish, Telapilia monsanbica. Neuroscience *49*, 237–246.

Turner, K.J., Hawkins, T.A., Yáñez, J., Anadón, R., Wilson, S.W., and Folgueira, M. (2016). Afferent Connectivity of the Zebrafish Habenulae. Front. Neural Circuits *10*, 30.

Wright, J., Campos, C., Herzog, T., Covasa, M., Czaja, K., and Ritter, R.C. (2011). Reduction of food intake by cholecystokinin requires activation of hindbrain NMDA-type glutamate receptors. Am. J. Physiol. - Regul. Integr. Comp. Physiol. *301*, 448–455.

Wullimann, M.F., and Mueller, T. (2004). Erratum: Teleostean and mammalian forebrains contrasted: Evidence from genes to behavior (Journal of Comparative Neurology (2004) 475 (143-162)). J. Comp. Neurol. *478*, 427–428.

Yamamoto, N., and Ito, H. (2005). Fiber connections of the anterior preglomerular nucleus in cyprinids with notes on telencephalic connections of the preglomerular complex. J. Comp. Neurol. *491*, 212–233.

Yáñez, J., Souto, Y., Piñeiro, L., Folgueira, M., and Anadón, R. (2017). Gustatory and general visceral centers and their connections in the brain of adult zebrafish: a carbocyanine dye tract-tracing study. J. Comp. Neurol. *525*, 333–362.

Yang, Y., Atasoy, D., and Sternson, S. (2011). Flip-flop memory circuit uses a synaptic AMPK-dependent positive feedback loop and is switched by hunger state. Appetite *57*, S47.

Yokobori, E., Azuma, M., Nishiguchi, R., Kang, K.S., Kamijo, M., Uchiyama, M., and Matsuda, K. (2012). Neuropeptide Y Stimulates Food Intake in the Zebrafish, Danio rerio. J. Neuroendocrinol. *24*, 766–773.

Yokogawa, T., Marin, W., Faraco, J., Pézeron, G., Appelbaum, L., Zhang, J., Rosa, F., Mourrain, P., and Mignot, E. (2007). Characterization of sleep in zebrafish and insomnia in hypocretin receptor mutants. PLoS Biol. *5*, 2379–2397.

Zhang, L., Hernandez-Sanchez, D., and Herzog, H. (2019). Regulation of Feeding-Related Behaviors by Arcuate Neuropeptide Y Neurons. Endocrinology *160*, 1411–1420.

ETHICS APPROVAL

All protocols used in this study were approved by Institutional Animal Ethics Committee of IISER Pune.

AVAILABILITY OF DATA AND MATERIAL

All data generated or analysed during this study are included in this published article. The raw data are available from the corresponding author on reasonable request.

CONFLICT OF INTEREST

The authors declare that they have no conflict of interest.

FUNDING

The study was supported by intramural support from IISER Pune to A.G. and a grant from the Department of Biotechnology, Govt. of India (BT/PR26241/GET/119/244/2017) to A.G.. D.B. was support by a fellowship from IISER Pune and A.M. was supported by a fellowship from the Council for Scientific and Industrial Research. The National Facility for Gene Function in Health and Disease (NFGFHD) at IISER Pune is supported by the Department of Biotechnology, Govt. of India (BT/INF/22/SP17358/2016).

AUTHOR CONTRIBUTIONS

Conceptualization: D.B., A.M., N.S. and A.G.; Investigation and formal analysis: D.B., A.M. and T.K.; Generation of preliminary data: D.W. and A.B.; Writing – original draft: D.B., A.M. and A.G.; Writing – review and editing: D.B., A.M., N.S. and A.G.; Funding Acquisition: A.G.. All authors gave final approval for publication and agree to be held accountable for the work performed therein.

ACKNOWLEDGMENTS

The authors thank Dr. G. Deshpande, Princeton University, Dr. S. Rath, IISER Pune and Dr. R. Rajan, IISER Pune for their critical reading of this manuscript and discussions. The Tg(NeuroD:GCaMP6f) line was a gift from Dr. V. Thirumalai, NCBS, Bengaluru. N. Tiwari, IISER Pune is acknowledged for contributing to the development of the feeding assay. The authors acknowledge the IISER Pune Microscopy Facility and the National Facility for Gene Function in Health and Disease (NFGFHD) at IISER Pune for access to equipment and infrastructure.

985 **FIGURE LEGENDS**

986 **Figure 1. CART neuropeptide regulates satiety in adult zebrafish.**

987 **(A)** The feeding drive as indicated by the cumulative number of biting attempts made
988 by fed and starved animals in 15 min bins (N=6 animals per group). **(B)**The
989 cumulative number of biting attempts made by starved fish intracerberoventicularly
990 injected with either vehicle or CART peptide (N=6 animals per group). **(C)**The
991 cumulative number of biting attempts made by starved fish icv injected with either
992 vehicle, glucose, CART antibodies or coinjected with immunoneutralising CART
993 antibodies (CART Ab) along with glucose (N= 5 for vehicle control and CART Ab
994 treated animals and N=6 for glucose and CART Ab + glucose treated animals). Data
995 are represented as cumulative biting attempts in 15 min bins over a 1-hour period
996 and compared using two-way ANOVA, with Bonferroni's post-hoc analysis for
997 significance in comparison with the glucose treated starved fish (error bars represent
998 ± SEM; ns, not significant; **p<0.01, ***p<0.001).

999

1000 **Figure 2. CART neuropeptide and satiety increases the activity of the**
1001 **dorsomedial telencephalon (Dm) neurons.**

1002 **(A,B)** Representative micrographs of Dm region from the transverse sections of the
1003 telencephalon showing p-ERK immunoreactive (p-ERK-ir) cells in starved fish icv
1004 injected with either vehicle or CART peptide. **(C)** The number of p-ERK-ir cells in Dm
1005 in starved fish icv injected with either vehicle or CART. The data are compared using
1006 the unpaired t-test with Welch's correction (N=6 animals per group; **p<0.01). **(D,E)**
1007 representative micrographs of Dm region from the transverse sections of the
1008 telencephalon showing p-ERK-ir cells under starved and fed conditions. **(F)** The

1009 number of p-ERK-ir cells in Dm under starved and fed states. The data are
1010 compared using the unpaired t-test with Welch's correction (N=6 animals per group).
1011 (**p<0.01, ***p<0.001). Scale bar: 50 μm. **(G)** The top view of zebrafish
1012 telencephalon with shaded region (dark red) indicating the entire dorsomedial
1013 telencephalon. The area bounded by dotted lines within dorsomedial telencephalon
1014 (light red) shows differential activity upon CART treatment and under fed/starved
1015 conditions. We refer to this subregion as Dm for the purposes of this study. **(H)** Side
1016 view of zebrafish brain with dark red area marking entire dorsomedial telencephalon.
1017 The region of our interest – within dorsomedial telencephalon - Dm (light red) is
1018 marked by dotted lines (a: marks the rostral limit of the region which shows
1019 differential activity; b: marks the plane of section shown in I; c: marks the caudal limit
1020 at the level of the anterior commissure (ac); the distance from a to c is ~250 μm). **(I)**
1021 A transverse section of telencephalon with the Dm region marked in light red colour.
1022 [ac, anterior commissure; Dp, posterior zone of dorsal telencephalon; EN,
1023 entopeduncular nucleus; Hy, hypothalamus; Ha, habenula; IOP, integrative olfactory
1024 pallium; MP, medial pallium; nLOT- nucleus of the lateral olfactory tract; OB,
1025 olfactory bulb; PMPa, posteromedial pallial nucleus; Sy, sulcus yipsiloniformis; TeO,
1026 optic tectum; Vd, dorsal nucleus of ventral telencephalic area; Vv, ventral nucleus of
1027 ventral telencephalic area]

1028

1029 **Figure 3. NMDAR signalling is necessary for CART-induced anorexia and**
1030 **increased activation of Dm neurons.**

1031 **(A)** The cumulative number of biting attempts made by starved zebrafish icv injected
1032 with either vehicle, CART peptide, AP5 or coinjected with AP5 and CART peptide.
1033 (N=6 animals per group). Data are represented as cumulative biting attempts in 15

1034 min bins over a 1-hour period and compared using two-way ANOVA, with
1035 Bonferroni's post-hoc analysis (error bars represent ±SEM; **p<0.01, ***p<0.001).
1036 **(B)** The number of p-ERK-ir cells in starved fish icv injected with either vehicle,
1037 CART, AP5 or coinjection of AP5 along with CART. The data are compared using
1038 two-way ANOVA, with Bonferroni's post-hoc analysis for significance in comparison
1039 with the CART treated starved fish (N=6 animals per group; ***p<0.001).

1040

1041 **Figure 4. CART-induced anorexia and activation of Dm neurons require PKA**
1042 **and PKC activity.**

1043 **(A)** The cumulative number of biting attempts made by starved fish icv injected with
1044 either vehicle, CART, PKAi or coinjection of PKAi along with CART. (N=6 animals
1045 per group). Data are represented as cumulative biting attempts in 15 min bins over a
1046 1-hour period and compared using two-way ANOVA, with Bonferroni's post-hoc
1047 analysis for significance in comparison with the CART treated starved fish (error bars
1048 represent ±SEM; ns, not significant; ***, p<0.001, **p<0.01). **(B)** The number of p-
1049 ERK-ir cells in starved fish icv injected with either vehicle, CART peptide, PKAi or
1050 coinjected with PKAi and CART peptide. Data are compared using two-way ANOVA,
1051 with Bonferroni's post-hoc analysis for significance in comparison with the CART
1052 treated starved fish (N=6 animals per group; ***, p< 0.001, **p<0.01). **(C)** The
1053 cumulative number of biting attempts made by starved fish icv injected with either
1054 vehicle, CART peptide, PKCi or coinjected with PKCi and CART peptide. (N=6
1055 animals per group). Data are represented as cumulative biting attempts in 15 min
1056 bins over a 1-hour period and compared using two-way ANOVA, with Bonferroni's
1057 post-hoc analysis for significance in comparison with the CART treated starved fish
1058 (error bars represent ±SEM; ***, p<0.001, **p<0.01). **(D)** The number of p-ERK-ir

1059 cells in starved fish icv injected with either vehicle, CART, PKCi or co-injection of
1060 PKCi along with CART. The data are compared using two-way ANOVA, with
1061 Bonferroni's post-hoc analysis for significance in comparison with the CART treated
1062 starved fish (N=6; ***, p< 0.001). **(E,F)** representative micrographs of one lobe of the
1063 Dm region from the transverse sections of the telencephalon showing phosphoNR1
1064 (Ser-897) (pNR1) immunoreactivity in starved fish icv injected with either CART
1065 peptide or co-injected with PKAi and PKCi along with CART peptide. **(G)**
1066 Quantification of mean pNR1 intensity per neuron (au: arbitrary units) in the Dm of
1067 starved fish icv injected with either vehicle and CART or co-injected with PKAi and
1068 PKCi along with CART peptideThe data were compared using unpaired t-test with
1069 Welch's correction (12253 cells in vehicle +CART group and 12015 cells in PKAi +
1070 PKCi + CART group; N=3 animals per group; ***, p< 0.001. Scale bar: 50 μm.)

1071

1072 **Figure 5. CART treatment enhances NMDAR function resulting in increased**
1073 **sensitivity of Dm neurons to glutamate.**

1074 **(A)** A timeline of the experimental protocol followed for all calcium imaging
1075 experiments using *ex-vivo* telencephalon preparations (details in Methods).
1076 Representative micrographs of neural activity (GCaMP6f fluorescence) in the Dm of
1077 vehicle (**B**) and CART peptide (**B'**) injected Tg(NeuroD:GCaMP6f) transgenic
1078 animals at the same time following stimulation with glutamate. The ventricle is
1079 towards the top of the image and C and R indicate caudal and rostral directions,
1080 respectively. Scale bar: 50 μm. In all graphs **(C, F, I)**, the traces represent relative
1081 change in fluorescence intensity (ΔF/F0) across time. The dark line represents the
1082 mean and the dotted lines denote the standard error of mean. The shaded
1083 rectangular box indicates the duration of glutamate presentation. (**C**) The change in

1084 fluorescence intensity (ΔF/F0) of Dm neurons in starved fish treated with either
1085 CART peptide (blue trace) or vehicle (brown trace). **(D)** The maximum response
1086 (ΔF/F0) and **(E)** the extent of the total response – AUC (area under the curve) for Dm
1087 neurons in starved fish treated with either CART peptide or vehicle. The data were
1088 compared using t-test with Welch's correction. (N=6 telencephalons per group,
1089 **p<0.01). **(F)** The change in fluorescence intensity (ΔF/F0) of Dm neurons in starved
1090 fish treated with either CART peptide (blue trace) or coinjected with AP5 and CART
1091 peptide (brown trace). **(G)** The maximum response (ΔF/F0) and **(H)** the extent of the
1092 total response of Dm neurons in starved fish treated with either CART peptide or
1093 coinjected with AP5 and CART. The data were compared using t-test with Welch's
1094 correction (N= 5 for CART and N=6 for AP5+CART telencephalons, *p<0.05). **(I)** The
1095 change in fluorescence intensity (ΔF/F0) of Dm neurons in starved fish treated with
1096 either CART peptide (blue trace) or coinjected with PKAi and PKCi along with CART
1097 peptide (brown trace). **(J)** The maximum response (ΔF/F0) and **(K)** the extent of the
1098 total response of Dm neurons in starved fish treated with either CART peptide or
1099 coinjected with PKAi, PKCi along with CART peptide. The data were compared using
1100 using t-test with Welch's correction (N=6 telencephalons per group, **p<0.01).

1101

1102 **Figure 6. Activity of Dm neurons increases in response to glucose.**

1103 **(A)** A timeline of the experimental protocol followed for calcium imaging experiments
1104 using *ex-vivo* whole brain preparations (details in Methods) **(B)** The traces represent
1105 relative change in fluorescence intensity (ΔF/F0) over time in response to glutamate.
1106 The thicker line represents mean while the associated finer lines indicate ± SEM.
1107 The shaded rectangular box indicates the duration of glutamate presentation.
1108 Response of Dm neurons in *ex-vivo* whole brain samples post 30' incubation with

1109 glucose (dark blue trace; post-glucose) is substantial compared to pre-glucose
1110 treatment (dark brown trace). Control experiments showed no response of Dm
1111 neurons before (light brown; pre-control) and after (light blue; post-control) 30 min
1112 incubation in glucose-free media. **(C)** The maximum response (ΔF/F0) and **(D)** the
1113 extent of the total response of Dm neurons pre- and post- incubation with
1114 glucose/glucose-free media. The data were analysed using one-way ANOVA and
1115 Tukey's multiple comparisons test (N=5 brains each each group, ***, p<0.001).

1116

1117 **Figure 7. NPY promotes food intake and reduces the activation of Dm neurons.**

1118 **(A)** The cumulative number of biting attempts made by starved fish icv injected with
1119 either vehicle or BIBP3226 (N= 6;, ***p<0.001). **(B)** The cumulative number of biting
1120 attempts made by fed fish icv injected with either vehicle or NPY (N=6; **p<0.01,
1121 ***p<0.001). Data are represented as cumulative biting attempts in 15 min bins over
1122 a 1-hour period and were compared using Two-way ANOVA, with Bonferroni's post-
1123 hoc analysis. **(C,D)** Representative micrographs of Dm region from the transverse
1124 sections across telencephalon showing p-ERK immunoreactive (p-ERK-ir) cells in
1125 fed fish icv injected with either vehicle or NPY **(E)** The number of p-ERK-ir cells in
1126 Dm of fed fish icv injected with either vehicle or NPY. The data were compared using
1127 unpaired t-test with Welch's correction (N=6; **p< 0.01). **(F,G)** representative
1128 micrographs of one lobe of Dm region from the transverse sections across
1129 telencephalon showing phosphoNR1 (pNR1) immunoreactivity in starved fish icv
1130 injected with either glucose or co-injected with NPY along with glucose **(H)**
1131 Quantification of mean pNR1 intensity per neuron (au: arbitrary units) in Dm in
1132 starved fish icv injected with either glucose or co-injected with NPY along with
1133 glucose. The data were compared using unpaired t-test with Welch's correction

1134 (12253 cells in vehicle+ glucose group and 11901 in NPY + glucose group; N=3; ***,
1135 p< 0.001) [Scale bar 50 μm] **(I)** The traces represent relative change in fluorescence
1136 intensity (ΔF/F0) over time in response to 75 μM glutamate. The dark line represents
1137 mean ± SEM with the dotted lines denoting the limits for standard error. The
1138 coloured rectangular box indicates the duration for which glutamate was presented.
1139 The response of Dm neurons in starved fish ICV injected glucose (blue trace) and
1140 co-injected with NPY along with glucose (brown trace). **(J)** The max (ΔF/F0) as well
1141 as **(K)** AUC of response of Dm neurons in starved fish icv injected glucose compared
1142 with the starved fish co-injected with NPY along with glucose. The data were
1143 analysed using t-test with Welch's correction. (N=6 telencephalons per group,
1144 *p<0.05).

1145

1146 **Figure 8 NPY inhibits adenylyl cyclase and activates of calcineurin to promote**
1147 **food intake.**

1148 **(A)** The cumulative number of biting attempts made by fed fishicv injected with either
1149 vehicle, NPY, FK506 or co-injection of FK506 along with NPY. (N=5 animals per
1150 group). Data are represented as cumulative biting attempts in 15 min bins over a 1-
1151 hour period and compared using Two-way ANOVA, with Bonferroni's post-hoc
1152 analysis for significance in comparison with the NPY treated fed fish(error bars
1153 represent ± SEM; *** p<0.001). **(B)** The number of p-ERK-ir cells in fed fish icv
1154 injected with either vehicle, NPY, FK506 or co-injection of FK506 along with NPY.
1155 Data were compared using Two-way ANOVA, with Bonferroni's post-hoc analysis for
1156 significance in comparison with the NPY treated fed fish (N=5; *** p< 0.001). **(C)** The
1157 cumulative number of biting attempts made by fed fishicv injected with either vehicle,
1158 NPY, Forskolin or co-injection of Forskolin along with NPY (N=5 animals per group).

1159 Data are represented as cumulative biting attempts in 15 min bins over a 1-hour
1160 period and were compared using Two-way ANOVA, with Bonferroni's post-hoc
1161 analysis for significance in comparison with the NPY treated fed fish (error bars
1162 represent ± SEM; *** $p<0.001$, *$p<0.05$). **(D)** The number of p-ERK-ir cells in fed fish
1163 icv injected with either vehicle, NPY, Forskolin or coinjection of Forskolin along with
1164 NPY. Data are compared using Two-way ANOVA, with Bonferroni's post-hoc
1165 analysis for significance in comparison with the NPY treated fed fish(N=5; ** $p<$
1166 0.01). **(E)** Schematic showing CART and NPY projections to Dm from interoceptive
1167 regions in zebrafish brain. [OB: olfactory bulb; EN: Entopeduncular nucleus; ac:
1168 anterior commissure; Ha: Habenula; Hy: Hypothalamus; TeO: Optic tectum] **(E')**
1169 Summary of modulatory changes induced by CART and NPY leading to a
1170 corresponding change in neural activity and food intake under fed and starved
1171 conditions, respectively. Under energy enriched conditions (Fed), CART signalling at
1172 the Dm is increased. CART activates PKA and PKC to increase the phosphorylation
1173 of NR1 subunit of NMDARs and thereby increases NMDAR activity in Dm neurons.
1174 CART mediated increase in Dm neuronal activity is correlated with a decrease in
1175 food intake in zebrafish. In contrast, under energy deprived conditions, NPY
1176 signalling at the Dm is increased. NPY acting via Y1R reduces PKA activity and
1177 activates calcineurin to decrease phosphorylation of NR1, in turn, decreasing
1178 NMDAR activity. NPY mediated reduction in Dm neuronal activity is correlated with
1179 increased food intake in zebrafish.

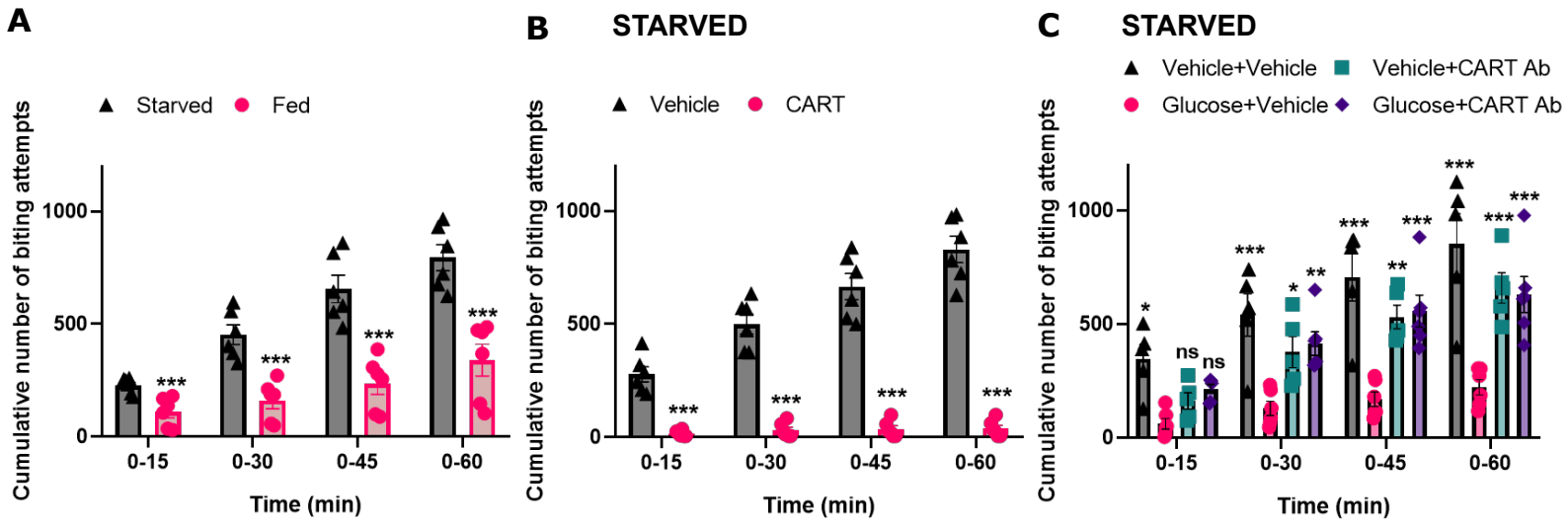
A
Starved
Fed
Cumulative number of biting attempts
1000
500
0
***
0-15
0-30
0-45
0-60
Time (min)
B
STARVED
Vehicle
CART
C
STARVED
Vehicle+Vehicle
Vehicle+CART Ab
Glucose+Vehicle
Glucose+CART Ab
ns
*
**

Figure 1

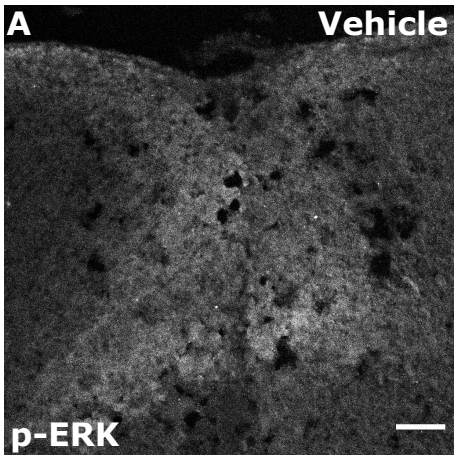
A
Vehicle
p-ERK

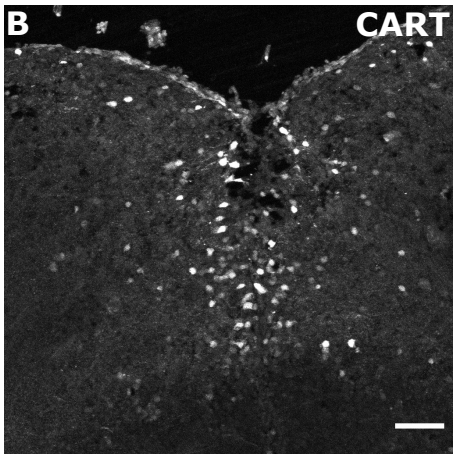
B
CART

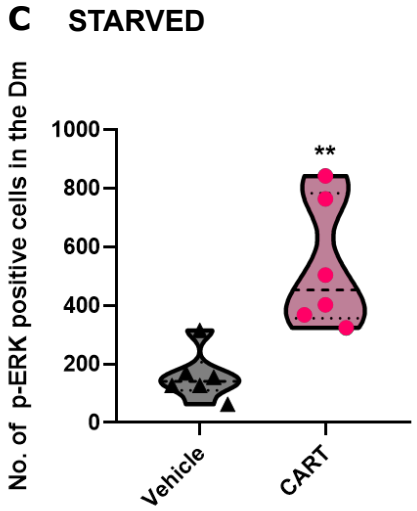
C
STARVED
No. of p-ERK positive cells in the Dm
1000
800
600
400
200
0
**
Vehicle
CART

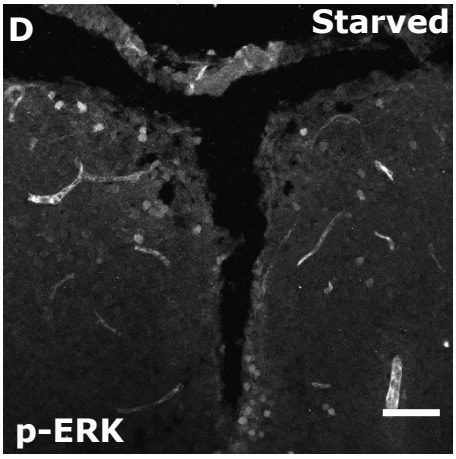
D
Starved
p-ERK

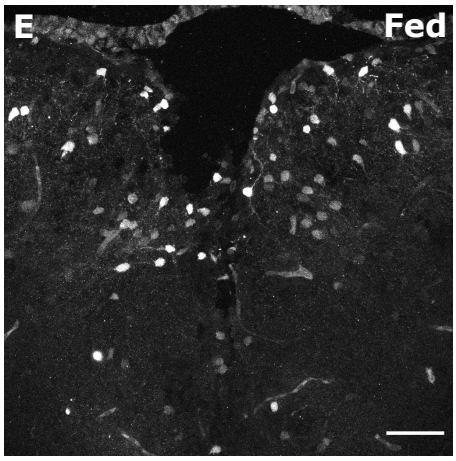
E
Fed

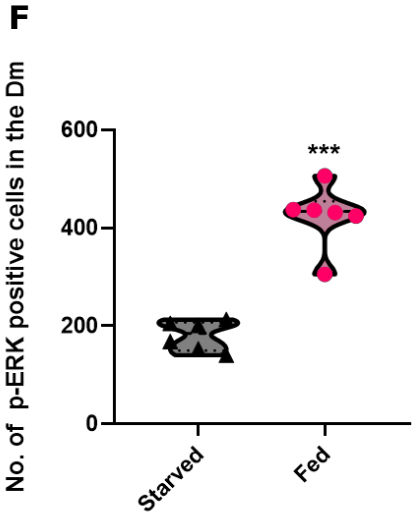
F
No. of p-ERK positive cells in the Dm
600
400
200
0
***
Starved
Fed

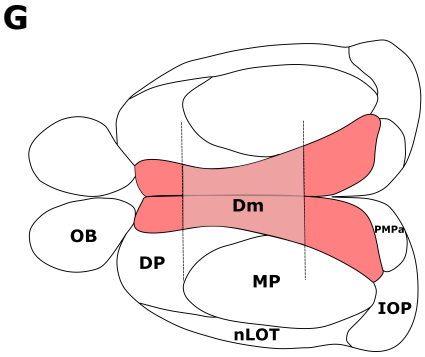
G
Dm
OB
DP
MP
PMPa
IOP
nLOT

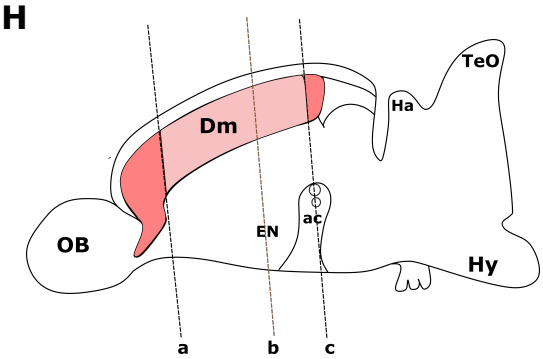
H
TeO
Ha
Dm
OB
EN
ac
Hy
a
b
c

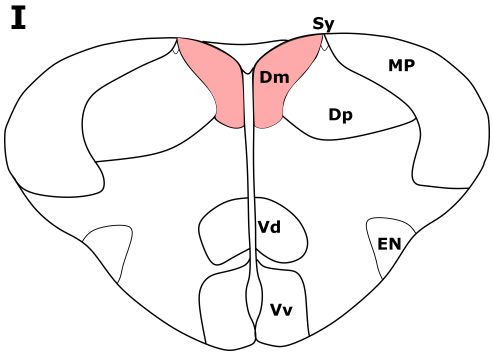
I
Sy
MP
Dm
Dp
Vd
EN
Vv

Figure 2

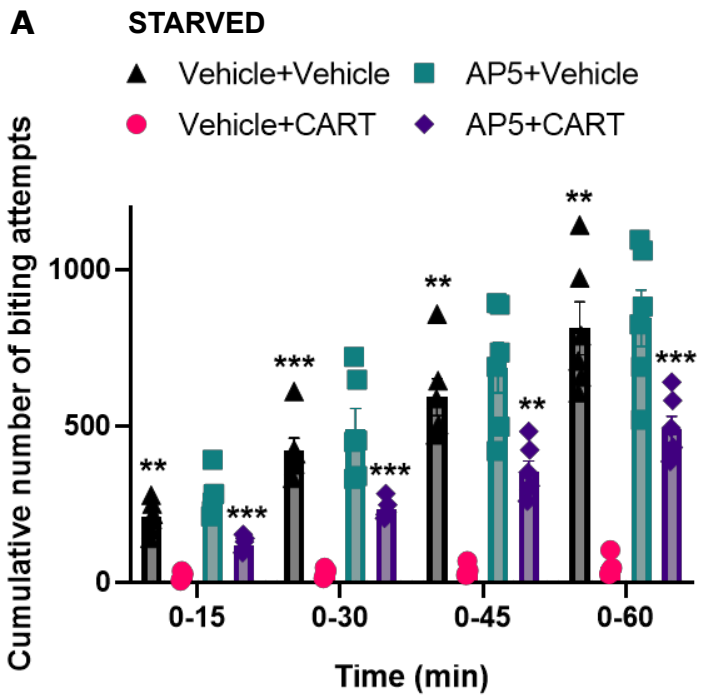
A
STARVED
Vehicle+Vehicle
AP5+Vehicle
Vehicle+CART
AP5+CART
Cumulative number of biting attempts
1000
500
0
**
***
***
**
***
**
**
***
0-15
0-30
0-45
0-60
Time (min)

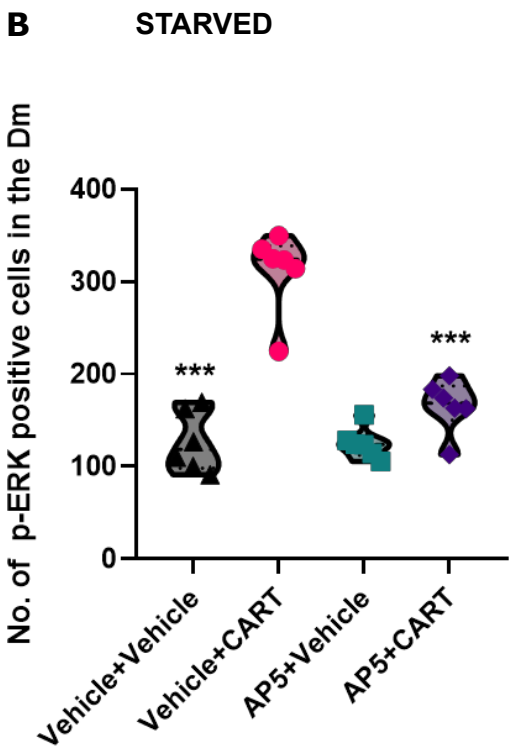
B
STARVED
No. of p-ERK positive cells in the Dm
400
300
200
100
0
***
***
Vehicle+Vehicle
Vehicle+CART
AP5+Vehicle
AP5+CART

Figure3

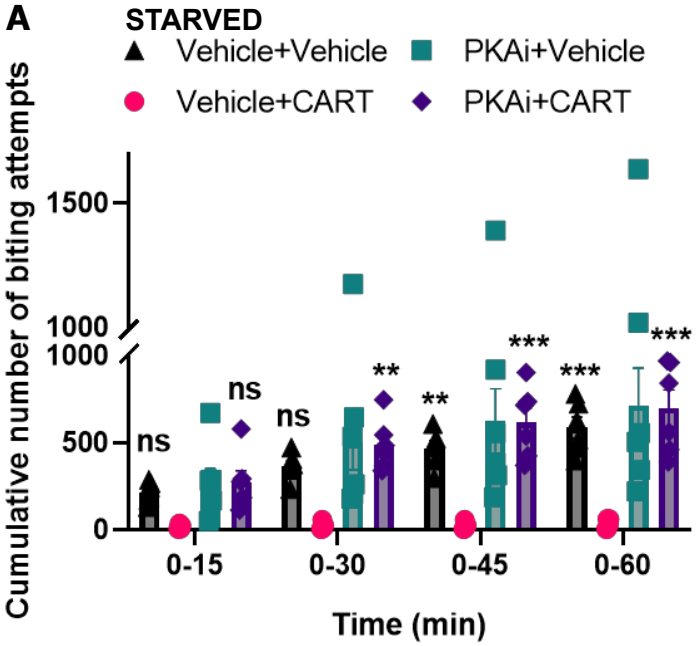
A
STARVED
Vehicle+Vehicle
PKAi+Vehicle
Vehicle+CART
PKAi+CART
Cumulative number of biting attempts
1500
1000
1000
500
0
ns
ns
ns
**
**
***
***
***
0-15
0-30
0-45
0-60
Time (min)

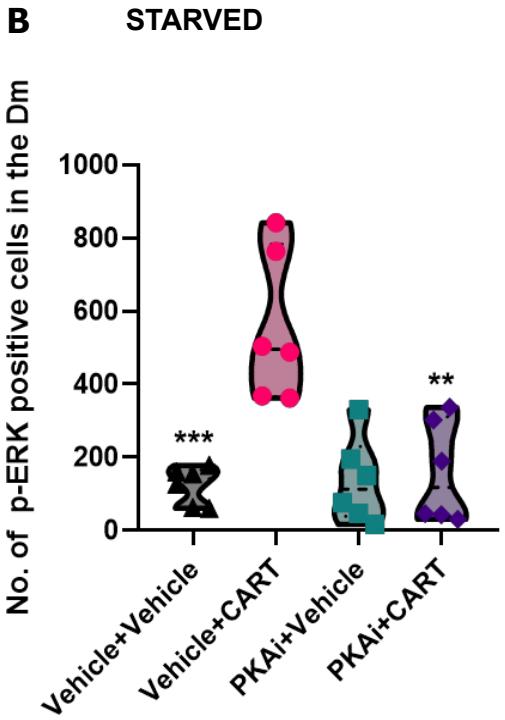
B
STARVED
No. of p-ERK positive cells in the Dm
1000
800
600
400
200
0
***
**
Vehicle+Vehicle
Vehicle+CART
PKAi+Vehicle
PKAi+CART

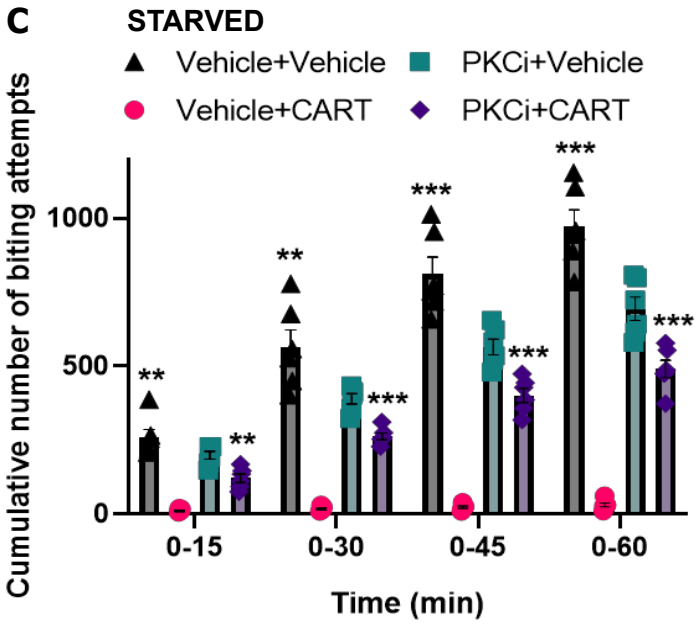
C
STARVED
Vehicle+Vehicle
PKCi+Vehicle
Vehicle+CART
PKCi+CART
Cumulative number of biting attempts
1000
500
0
**
**
**
***
***
***
***
***
0-15
0-30
0-45
0-60
Time (min)

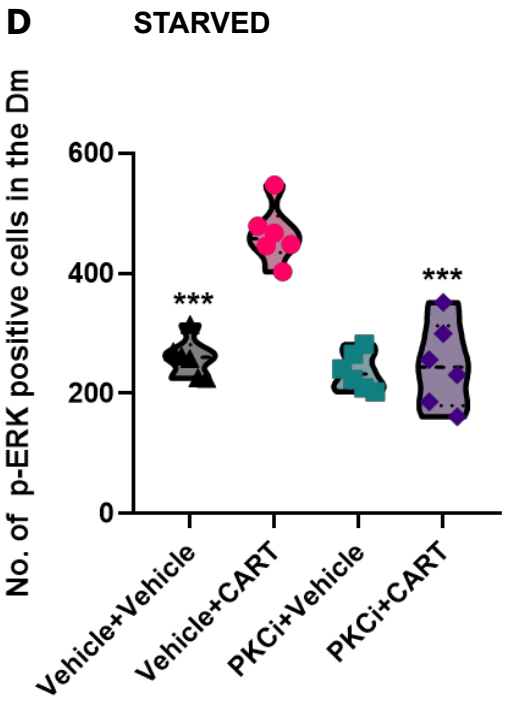
D
STARVED
No. of p-ERK positive cells in the Dm
600
400
200
0
***
***
Vehicle+Vehicle
Vehicle+CART
PKCi+Vehicle
PKCi+CART

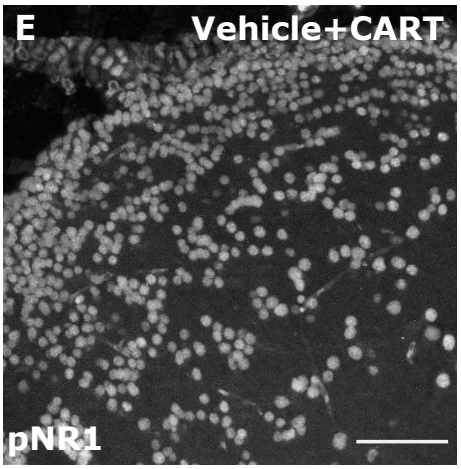
E
Vehicle+CART
pNR1

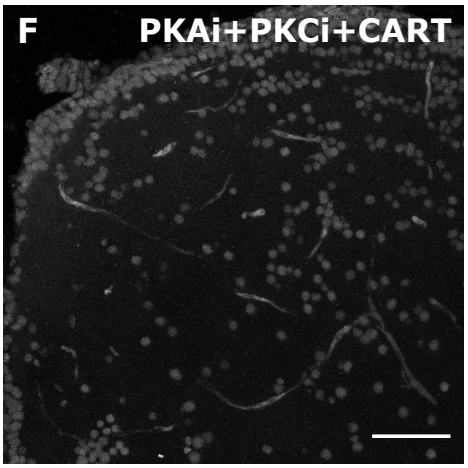
F
PKAi+PKCi+CART

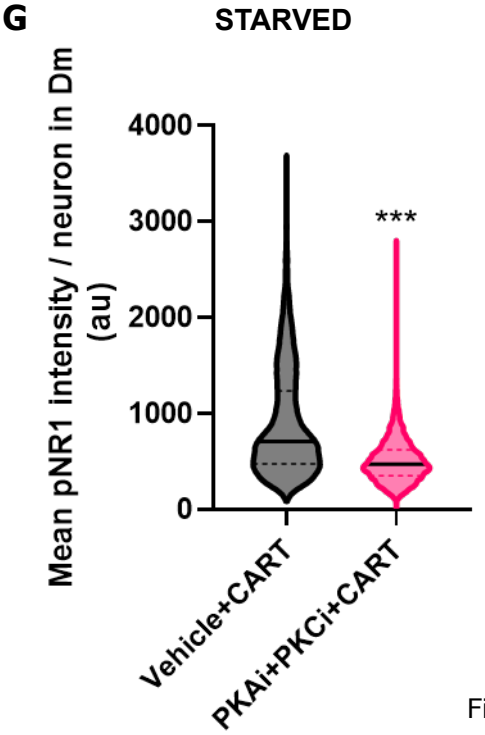
G
STARVED
Mean pNR1 intensity / neuron in Dm (au)
4000
3000
2000
1000
0
***
Vehicle+CART
PKAi+PKCi+CART

Figure4

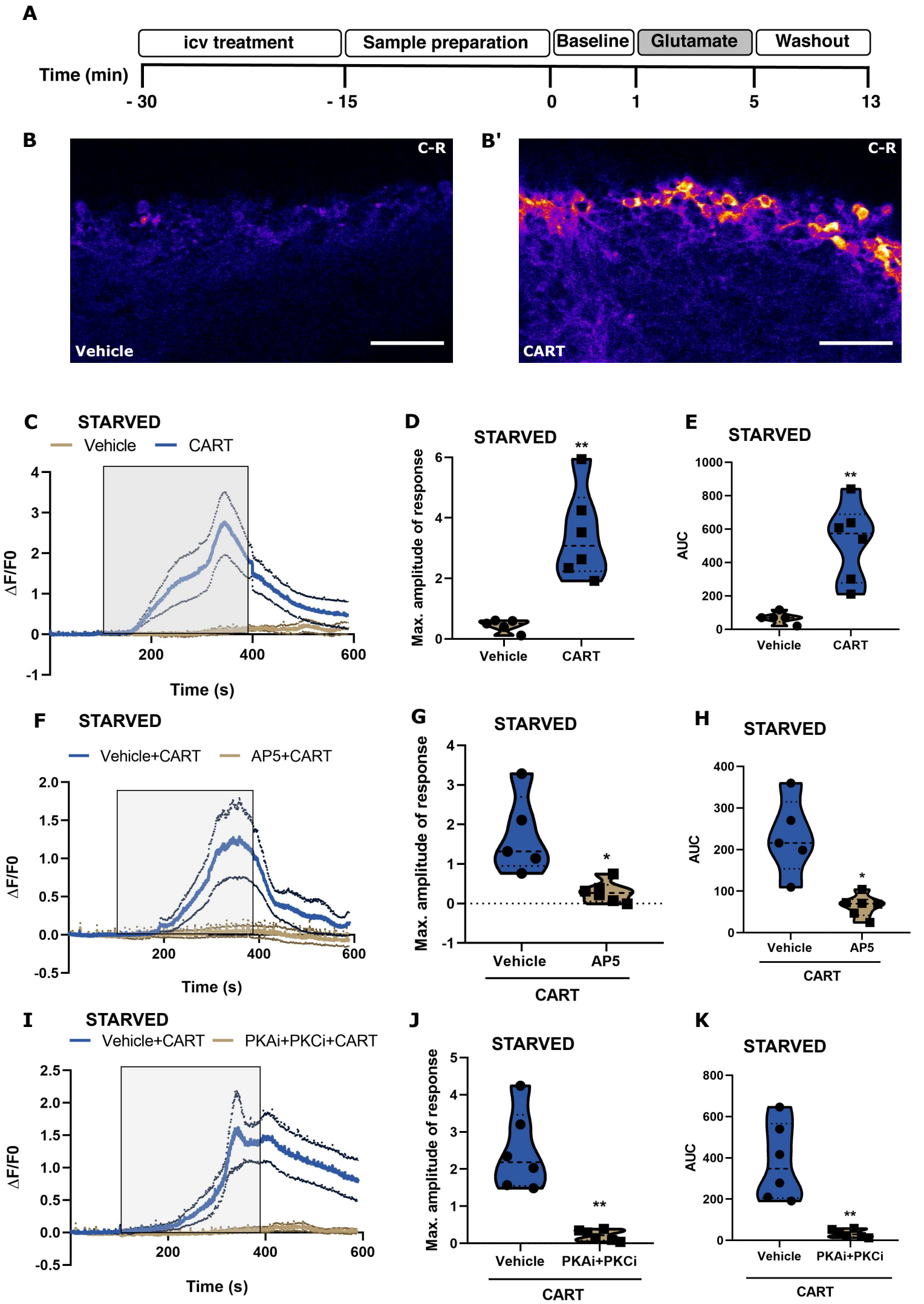
A
icv treatment
Sample preparation
Baseline
Glutamate
Washout
Time (min)
- 30
- 15
0
1
5
13
B
C-R
Vehicle
B'
C-R
CART
C
STARVED
Vehicle
CART
ΔF/F0
Time (s)
D
STARVED
Max. amplitude of response
Vehicle
CART
E
STARVED
AUC
Vehicle
CART
F
STARVED
Vehicle+CART
AP5+CART
ΔF/F0
Time (s)
G
STARVED
Max. amplitude of response
Vehicle
AP5
CART
H
STARVED
AUC
Vehicle
AP5
CART
I
STARVED
Vehicle+CART
PKAi+PKCi+CART
ΔF/F0
Time (s)
J
STARVED
Max. amplitude of response
Vehicle
PKAi+PKCi
CART
K
STARVED
AUC
Vehicle
PKAi+PKCi
CART

Figure 5

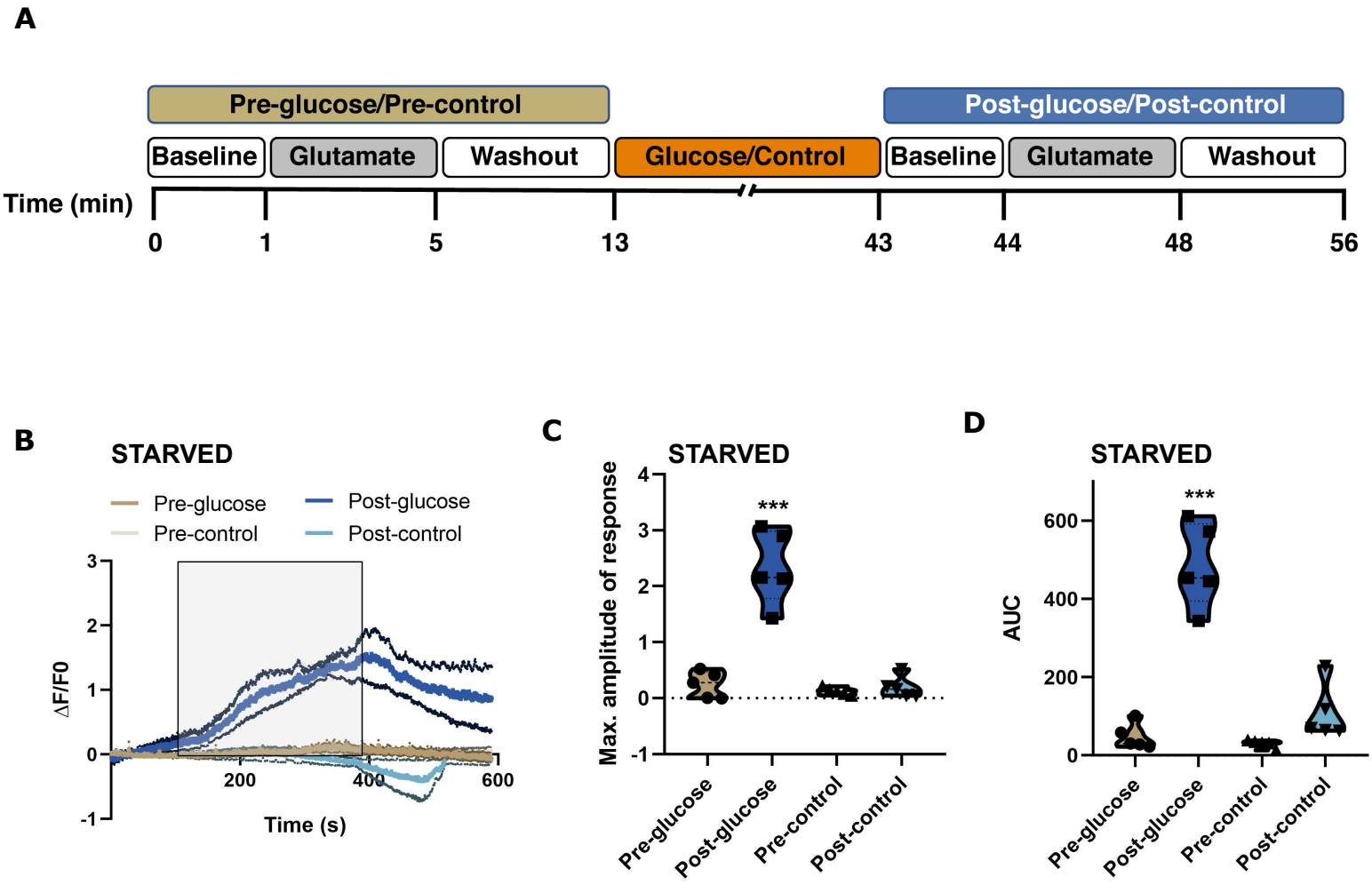
A
Pre-glucose/Pre-control
Post-glucose/Post-control
Baseline
Glutamate
Washout
Glucose/Control
Baseline
Glutamate
Washout
Time (min)
0
1
5
13
43
44
48
56
B
STARVED
Pre-glucose
Pre-control
Post-glucose
Post-control
ΔF/F0
Time (s)
C
STARVED
Max. amplitude of response
***
Pre-glucose
Post-glucose
Pre-control
Post-control
D
STARVED
AUC
***
Pre-glucose
Post-glucose
Pre-control
Post-control

Figure 6

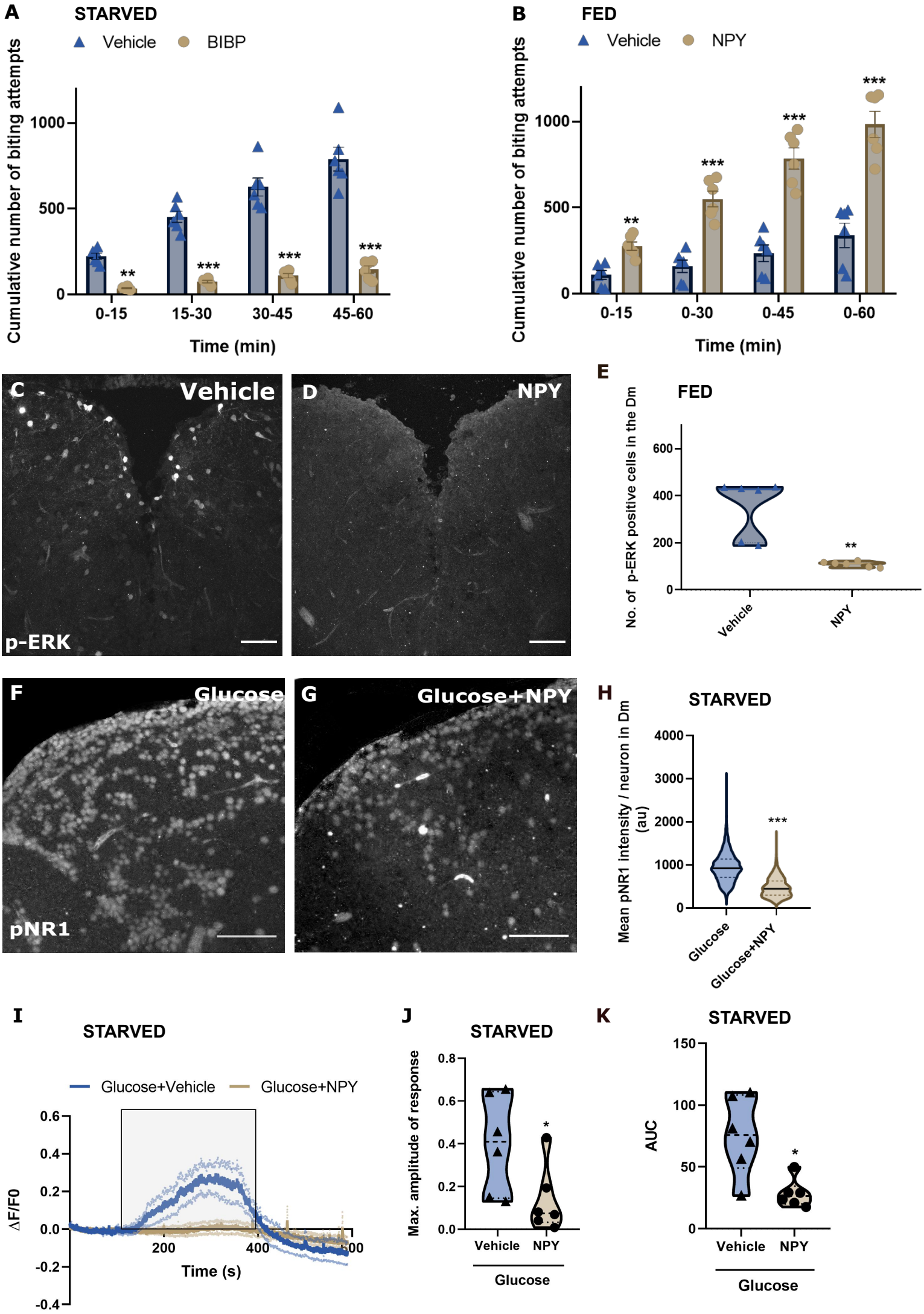
A
STARVED
Vehicle
BIBP
Cumulative number of biting attempts
1000
500
0
**
***
***
***
0-15
15-30
30-45
45-60
Time (min)
B
FED
Vehicle
NPY
Cumulative number of biting attempts
1000
500
0
**
***
***
***
0-15
0-30
0-45
0-60
Time (min)
C
Vehicle
p-ERK
D
NPY
E
FED
No. of p-ERK positive cells in the Dm
600
400
200
0
**
Vehicle
NPY
F
Glucose
pNR1
G
Glucose+NPY
H
STARVED
Mean pNR1 intensity / neuron in Dm (au)
4000
3000
2000
1000
0
***
Glucose
Glucose+NPY
I
STARVED
Glucose+Vehicle
Glucose+NPY
ΔF/F0
0.6
0.4
0.2
0.0
-0.2
-0.4
200
400
Time (s)
J
STARVED
Max. amplitude of response
0.8
0.6
0.4
0.2
0.0
*
Vehicle
NPY
Glucose
K
STARVED
AUC
150
100
50
0
*
Vehicle
NPY
Glucose

Figure 7

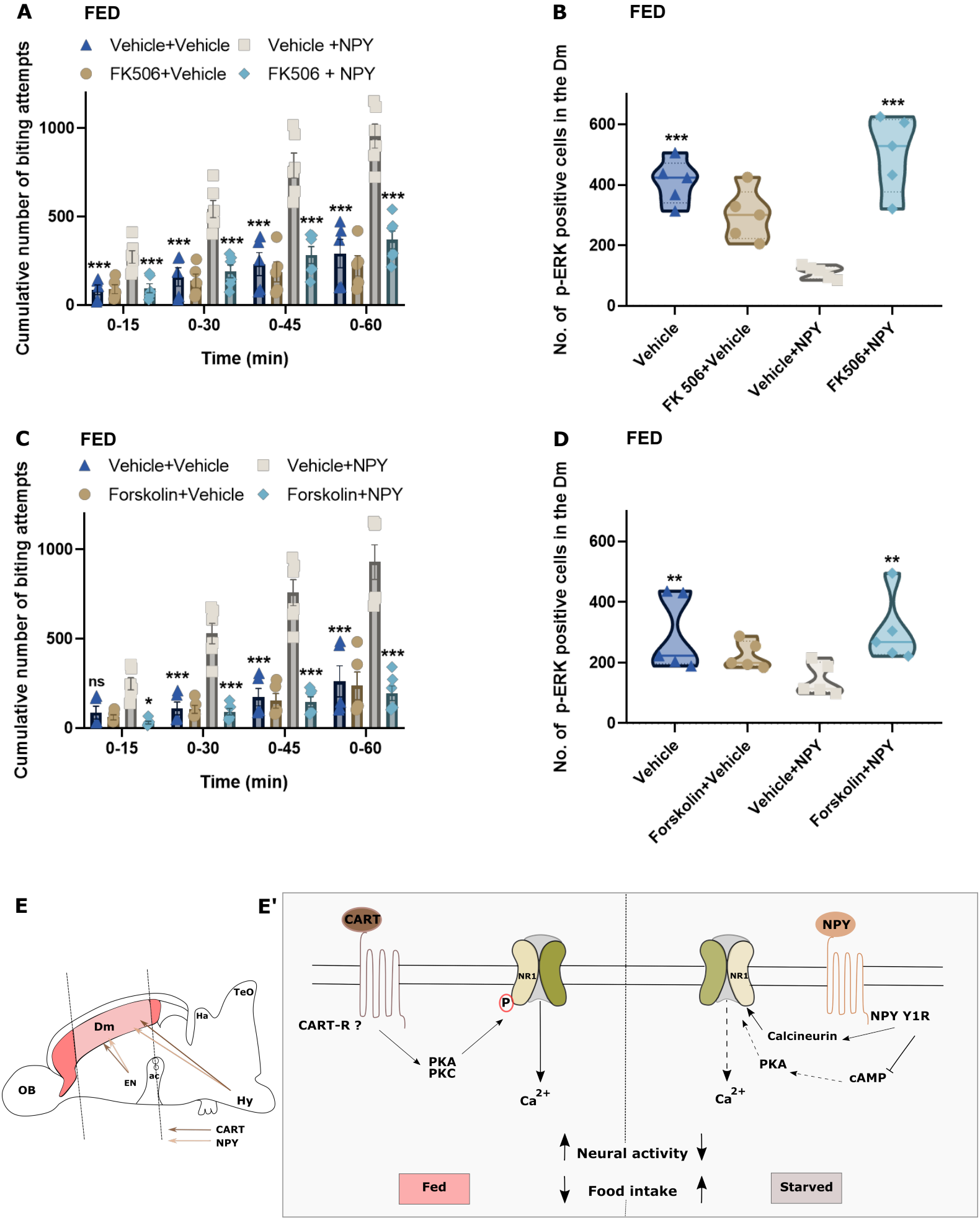
A
FED
Vehicle+Vehicle
Vehicle +NPY
FK506+Vehicle
FK506 + NPY
Cumulative number of biting attempts
1000
500
0
0-15
0-30
0-45
0-60
Time (min)
B
FED
No. of p-ERK positive cells in the Dm
600
400
200
0
Vehicle
FK 506+Vehicle
Vehicle+NPY
FK506+NPY
C
FED
Vehicle+Vehicle
Vehicle+NPY
Forskolin+Vehicle
Forskolin+NPY
Cumulative number of biting attempts
1000
500
0
ns
0-15
0-30
0-45
0-60
Time (min)
D
FED
No. of p-ERK positive cells in the Dm
600
400
200
0
Vehicle
Forskolin+Vehicle
Vehicle+NPY
Forskolin+NPY
E
TeO
Ha
Dm
OB
EN
ac
Hy
CART
NPY
E'
CART
NPY
NR1
P
CART-R ?
PKA
PKC
Ca2+
Calcineurin
PKA
cAMP
NPY Y1R
Neural activity
Food intake
Fed
Starved

Figure 8